Measurement of the correlation between flow harmonics of different order in lead-lead collisions at $\sqrt{s_{NN}} = 2.76$ TeV with the ATLAS detector

G. Aad *et al.**
(ATLAS Collaboration)

Correlations between the elliptic or triangular flow coefficients v_m ($m = 2$ or 3) and other flow harmonics v_n ($n = 2$ to 5) are measured using $\sqrt{s_{NN}} = 2.76$ TeV Pb + Pb collision data collected in 2010 by the ATLAS experiment at the LHC, corresponding to an integrated luminosity of 7 μb^{-1}. The v_m-v_n correlations are measured in midrapidity as a function of centrality, and, for events within the same centrality interval, as a function of event ellipticity or triangularity defined in a forward rapidity region. For events within the same centrality interval, v_3 is found to be anticorrelated with v_2 and this anticorrelation is consistent with similar anticorrelations between the corresponding eccentricities, ϵ_2 and ϵ_3. However, it is observed that v_4 increases strongly with v_2, and v_5 increases strongly with both v_2 and v_3. The trend and strength of the v_m-v_n correlations for $n = 4$ and 5 are found to disagree with ϵ_m-ϵ_n correlations predicted by initial-geometry models. Instead, these correlations are found to be consistent with the combined effects of a linear contribution to v_n and a nonlinear term that is a function of v_2^2 or of $v_2 v_3$, as predicted by hydrodynamic models. A simple two-component fit is used to separate these two contributions. The extracted linear and nonlinear contributions to v_4 and v_5 are found to be consistent with previously measured event-plane correlations.

I. INTRODUCTION

Heavy-ion collisions at the Relativistic Heavy Ion Collider (RHIC) and the Large Hadron Collider (LHC) create hot and dense matter that is thought to be composed of strongly coupled quarks and gluons. The distribution of this matter in the transverse plane is both nonuniform in density and asymmetric in shape [1,2]. The matter expands under large pressure gradients, which transfer the inhomogeneous initial condition into azimuthal anisotropy of produced particles in momentum space [3,4]. Hydrodynamic models are used to understand the space-time evolution of the matter by comparing predictions with the measured azimuthal anisotropy [5–7]. The success of these models in describing the anisotropy of particle production in heavy-ion collisions at RHIC and the LHC [8–14] places significant constraints on the transport properties (such as the ratio of shear viscosity to entropy density) and initial conditions of the produced matter [15–20].

The azimuthal anisotropy of the particle production in each event can be characterized by a Fourier expansion of the corresponding probability distribution $P(\phi)$ in azimuthal angle ϕ [3,21],

$$P(\phi) = \frac{1}{2\pi}\left\{1 + \sum_{n=1}^{\infty}(\mathbf{v}_n e^{-in\phi} + [\mathbf{v}_n e^{-in\phi}]^*)\right\},$$
$$\mathbf{v}_n = v_n e^{in\Phi_n}, \qquad (1)$$

where v_n and Φ_n are the magnitude and phase (also known as the event plane or EP), respectively, of the nth-order harmonic flow, and $P(\phi)$ is real by construction. The presence of harmonic flow has been related to various moments of shape configurations of the initially produced fireball. These moments are described by the eccentricity vector $\boldsymbol{\epsilon}_n$ calculated from the transverse positions (r,ϕ) of the participating nucleons relative to their center of mass [4,16],

$$\boldsymbol{\epsilon}_n = \epsilon_n e^{in\Psi_n} = -\frac{\langle r^n e^{in\phi}\rangle}{\langle r^n\rangle}, \qquad (2)$$

where $\langle\cdots\rangle$ denotes an average over the transverse position of all participating nucleons and ϵ_n and Ψ_n (also known as the participant plane or PP) represent the magnitude and orientation of the eccentricity vector, respectively. The eccentricity vectors characterize the spatial anisotropy of the initially produced fireball, which drives the flow harmonics in the final state.

According to hydrodynamic model calculations, elliptic flow $\mathbf{v}_2$ and triangular flow $\mathbf{v}_3$ are the dominant harmonics, and they are driven mainly by the ellipticity vector $\boldsymbol{\epsilon}_2$ and triangularity vector $\boldsymbol{\epsilon}_3$ of the initially produced fireball [22,23]:

$$v_2 e^{i2\Phi_2} \propto \epsilon_2 e^{i2\Psi_2}, \quad v_3 e^{i3\Phi_3} \propto \epsilon_3 e^{i3\Psi_3}. \qquad (3)$$

This proportionality is often quantified by a ratio

$$k_n = v_n/\epsilon_n, \quad n = 2 \text{ or } 3, \qquad (4)$$

where the linear response coefficients k_n are found to be independent of the magnitude of ϵ_n but change with centrality [22,24].

The origin of higher-order ($n > 3$) harmonics is more complicated; they arise from both ϵ_n and nonlinear mixing of lower-order harmonics [20,23,25]. For example, an analytical calculation shows that the v_4 signal comprises a term proportional to ϵ_4 (linear response term) and a leading nonlinear term

---

that is proportional to ϵ_2^2 [23,26],

$$
\begin{aligned}
v_4 e^{i4\Phi_4} &= a_0\,\epsilon_4 e^{i4\Psi_4} + a_1\,(\epsilon_2 e^{i2\Psi_2})^2 + \cdots \\
&= c_0\,e^{i4\Psi_4} + c_1\,(v_2 e^{i2\Phi_2})^2 + \cdots ,
\end{aligned}
\tag{5}
$$

where the second line of the equation follows from Eq. (3), $c_0 = a_0\epsilon_4$ denotes the linear component of v_4, and coefficients a_0, a_1, and c_1 are weak functions of centrality. The nonlinear contribution from v_2 is responsible for the strong centrality dependence of the correlation between Φ_2 and Φ_4 observed by the ATLAS Collaboration [14] in Pb + Pb collisions. In a similar manner, the v_5 signal comprises a linear component proportional to ϵ_5 and a leading nonlinear term involving v_2 and v_3 [23,26]:

$$
\begin{aligned}
v_5 e^{i5\Phi_5} &= a_0\epsilon_5 e^{i5\Psi_5} + a_1\epsilon_2 e^{i2\Psi_2}\epsilon_3 e^{i3\Psi_3} + \cdots \\
&= c_0 e^{i5\Psi_5} + c_1 v_2 v_3 e^{i(2\Phi_2+3\Phi_3)} + \cdots .
\end{aligned}
\tag{6}
$$

This decomposition of the v_5 signal explains the measured EP correlation involving Φ_2, Φ_3, and Φ_5 [14].

Owing to fluctuations of nucleon positions in the initial state, ϵ_n and v_n vary from event to event, which can be described by probability distributions $p(\epsilon_n)$ and $p(v_n)$. Recent measurements by the ATLAS Collaboration [13] show that the distributions $p(v_n)$ are very broad: Even for events in a very narrow centrality interval, v_2 and v_3 can fluctuate from zero to several times their mean values. If events with different v_2 or v_3 values could be selected cleanly, one would be able to control directly the relative sizes of the linear and nonlinear contributions to v_4 and v_5 in Eqs. (5) and (6) and hence provide an independent method of separating these two contributions. Such an event-shape selection method has been proposed in Refs. [27,28], where events in a narrow centrality interval are further classified according to the observed ellipticity or triangularity in a forward rapidity region. These quantities are estimated from the "flow vector" q_m ($m = 2$ and 3), as described in Sec. IV A. This classification gives events with similar multiplicity but with very different ellipticity or triangularity. By measuring the v_n and v_m in a different rapidity window for each q_m event class, the differential correlation between v_m and v_n can be obtained in an unbiased way for each centrality interval, which allows the separation of the linear and nonlinear components in v_4 and v_5. The extracted linear component of v_4 and v_5 can then be used to understand the collective response of the medium to the initial eccentricity of the same order, using an approach similar to Eq. (4).

In addition to separating the linear and nonlinear effects, the correlation between v_m and v_n is also sensitive to any differential correlation between ϵ_m and ϵ_n in the initial state. One example is the strong anticorrelation between ϵ_2 and ϵ_3 predicted by the Monte Carlo (MC) Glauber model [28,29]. A recent transport-model calculation shows that this correlation survives the collective expansion and appears as a similar anticorrelation between v_2 and v_3 [28].

In this paper, the correlations between two flow harmonics of different order are studied using the event-shape selection method. The ellipticity or triangularity of the events is selected based on the q_2 or q_3 signal in the forward pseudorapidity

range of $3.3 < |\eta| < 4.8$.[1] The values of v_n for $n = 2$ to 5 are then measured at midrapidity $|\eta| < 2.5$ using a two-particle correlation method, and the correlations between two flow harmonics are obtained. The procedure for obtaining v_n in this analysis is identical to that used in a previous ATLAS publication [11], which is also based on the same data set. The main difference is that, in this analysis, the events are classified both by their centrality and by the observed q_2 or q_3 at forward pseudorapidity. Most systematic uncertainties are common to the two analyses.

II. ATLAS DETECTOR AND TRIGGER

The ATLAS detector [30] provides nearly full solid-angle coverage of the collision point with tracking detectors, calorimeters, and muon chambers. All of these are well suited for measurements of azimuthal anisotropies over a large pseudorapidity range. This analysis primarily uses two subsystems: the inner detector (ID) and the forward calorimeter (FCal). The ID is contained within the 2-T field of a superconducting solenoid magnet and measures the trajectories of charged particles in the pseudorapidity range $|\eta| < 2.5$ and over the full azimuth. A charged particle passing through the ID traverses typically three modules of the silicon pixel detector (Pixel), four double-sided silicon strip modules of the semiconductor tracker (SCT), and a transition radiation tracker for $|\eta| < 2$. The FCal consists of three sampling layers, longitudinal in shower depth, and covers $3.2 < |\eta| < 4.9$. The energies in the FCal are reconstructed and grouped into towers with segmentation in pseudorapidity and azimuthal angle of $\Delta\eta \times \Delta\phi \approx 0.2 \times 0.2$. In heavy-ion collisions, the FCal is used mainly to measure the event centrality and EPs [11,31]. In this analysis it is also used to classify the events in terms of q_2 or q_3 in the forward rapidity region.

The minimum-bias trigger used for this analysis requires signals in two zero-degree calorimeters (ZDCs) or either of the two minimum-bias trigger scintillator (MBTS) counters. The ZDCs are positioned at ± 140 m from the collision point, detecting neutrons and photons with $|\eta| > 8.3$, and the MBTS covers $2.1 < |\eta| < 3.9$ on each side of the nominal interaction point. The ZDC trigger thresholds on each side are set below the peak corresponding to a single neutron. A timing requirement based on signals from each side of the MBTS is imposed to remove beam backgrounds.

III. EVENT AND TRACK SELECTION

This analysis is based on approximately 7 $\mu\mathrm{b}^{-1}$ of Pb + Pb data collected in 2010 at the LHC with a nucleon-nucleon center-of-mass energy $\sqrt{s_{NN}} = 2.76$ TeV. The off-line event

---

[1]ATLAS uses a right-handed coordinate system with its origin at the nominal interaction point (IP) in the center of the detector and the z axis along the beam pipe. The x axis points from the IP to the center of the LHC ring, and the y axis points upward. Cylindrical coordinates (r,ϕ) are used in the transverse plane, ϕ being the azimuthal angle around the beam pipe. The pseudorapidity is defined in terms of the polar angle θ as $\eta = -\ln\tan(\theta/2)$.

TABLE I. The list of centrality intervals and associated values of the average number of participating nucleons N_{part} used in this analysis. The systematic uncertainties are taken from Ref. [32].

Centrality (%)	0–5	5–10	10–15	15–20	20–25	25–30	30–35
N_{part}	382 ± 2	330 ± 3	282 ± 4	240 ± 4	203 ± 4	170 ± 4	142 ± 4
Centrality (%)	35–40	40–45	45–50	50–55	55–60	60–65	65–70
N_{part}	117 ± 4	95 ± 4	76 ± 4	60 ± 3	46 ± 3	35 ± 3	25 ± 2

selection requires a reconstructed vertex and a time difference $|\Delta t| < 3$ ns between signals in the MBTS trigger counters on either side of the interaction point to suppress noncollision backgrounds. A coincidence between the ZDCs at forward and backward pseudorapidity is required to reject a variety of background processes, while maintaining high efficiency for inelastic processes. Events satisfying these conditions are further required to have a reconstructed primary vertex with $|z_{vtx}| < 150$ mm from the nominal center of the ATLAS detector. About 48×10^6 events pass the requirements.

The Pb + Pb event centrality [32] is characterized using the total transverse energy (ΣE_T) deposited in the FCal over the pseudorapidity range $3.2 < |\eta| < 4.9$ at the electromagnetic energy scale [33]. From an analysis of this distribution after all trigger and event-selection requirements, the fraction of the inelastic cross section sampled is estimated to be $98 \pm 2\%$. The uncertainty associated with the centrality definition is evaluated by varying the effect of trigger and event selection inefficiencies as well as background rejection requirements in the most peripheral FCal ΣE_T interval [32]. The FCal ΣE_T distribution is divided into a set of 5% percentile bins. A centrality interval refers to a percentile range, starting at 0% relative to the most central collisions. Thus, the 0%–5% centrality interval corresponds to the most central 5% of the events. An MC Glauber analysis [32,34] is used to estimate the average number of participating nucleons, N_{part}, for each centrality interval. These are summarized in Table I. Following the convention of heavy-ion analyses, the centrality dependence of the results in this paper is presented as a function of N_{part}.

The harmonic flow coefficients v_n are measured using tracks in the ID that are required to have transverse momentum $p_T > 0.5$ GeV and $|\eta| < 2.5$. At least nine hits in the silicon detectors are required for each track, with no missing Pixel hits and not more than one missing SCT hit, taking into account the effects of known dead modules. In addition, the point of closest approach of the track is required to be within 1 mm of the primary vertex in both the transverse and the longitudinal directions [31]. The efficiency $\epsilon(p_T, \eta)$ of the track reconstruction and track selection requirements is evaluated using simulated Pb + Pb events produced with the HIJING event generator (version 1.38b) [35]. The generated particles in each event are rotated in azimuthal angle according to the procedure described in Ref. [36] to give harmonic flow consistent with previous ATLAS measurements [11,31]. The response of the detector is simulated using GEANT4 [37,38] and the resulting events are reconstructed with the same algorithms that are applied to the data. The absolute efficiency increases with p_T by 7% between 0.5 and 0.8 GeV and varies only weakly for $p_T > 0.8$ GeV. However, the efficiency varies more strongly

with η and event multiplicity [31]. For $p_T > 0.8$ GeV, it ranges from 72% at $\eta \approx 0$ to 57% for $|\eta| > 2$ in peripheral collisions, while it ranges from 72% at $\eta \approx 0$ to about 42% for $|\eta| > 2$ in central collisions.

IV. DATA ANALYSIS

A. Event-shape selection

The ellipticity or triangularity in each event is characterized by the so-called "flow vector" calculated from the transverse energy (E_T) deposited in the FCal [14,39],

$$\boldsymbol{q}_m = q_m e^{im\Psi_m^{obs}} = \frac{\Sigma w_j e^{-im\phi_j}}{\Sigma w_j} - \langle \boldsymbol{q}_m \rangle_{evts}, \quad m = 2 \text{ or } 3, \tag{7}$$

where the weight w_j is the E_T of the jth tower at azimuthal angle ϕ_j in the FCal. Subtraction of the event-averaged centroid $\langle \boldsymbol{q}_m \rangle_{evts}$ in Eq. (7) removes biases due to detector effects [40]. The angles Ψ_m^{obs} are the observed EPs, which fluctuate around the true EPs Φ_m owing to the finite number of particles in an event. A standard technique [41] is used to remove the small residual nonuniformities in the distribution of Ψ_m^{obs}. These procedures are identical to those used in several previous flow analyses [11,13,14,40]. To reduce the detector nonuniformities at the edge of the FCal, only the FCal towers whose centroids fall within the interval $3.3 < |\eta| < 4.8$ are used.

The $\boldsymbol{q}_m$ defined above is insensitive to the energy scale in the calorimeter. In the limit of infinite multiplicity, it approaches the E_T-weighted single-particle flow:

$$\boldsymbol{q}_m \rightarrow \int E_T \boldsymbol{v}_m(E_T) dE_T \bigg/ \int E_T dE_T. \tag{8}$$

Hence, the q_m distribution is expected to follow closely the v_m distribution, except that it is smeared owing to the finite number of particles. Figure 1 shows the distributions of q_2 and q_3 in the 0%–1% most central collisions. These events are first divided into ten q_m intervals with equal number of events. Because the intervals at the highest and lowest q_m values cover much broader ranges, they are further divided into 5 and 2 smaller intervals, respectively, resulting in a total of 15 q_m intervals containing certain fractions of events. Starting at the low end of the q_m distribution, there are 2 intervals containing a fraction 0.05 (labeled 0.95–1 and 0.9–0.95), 8 intervals containing 0.1, 3 containing 0.025, 1 containing 0.015, and 1 containing 0.01 (this last interval spans the highest values of q_m). These 15 intervals are defined separately for each 1% centrality interval and are then grouped together to form wider centrality intervals used in this analysis (see Table I). For example, the first q_m interval for the 0%–5% centrality interval is the sum of the
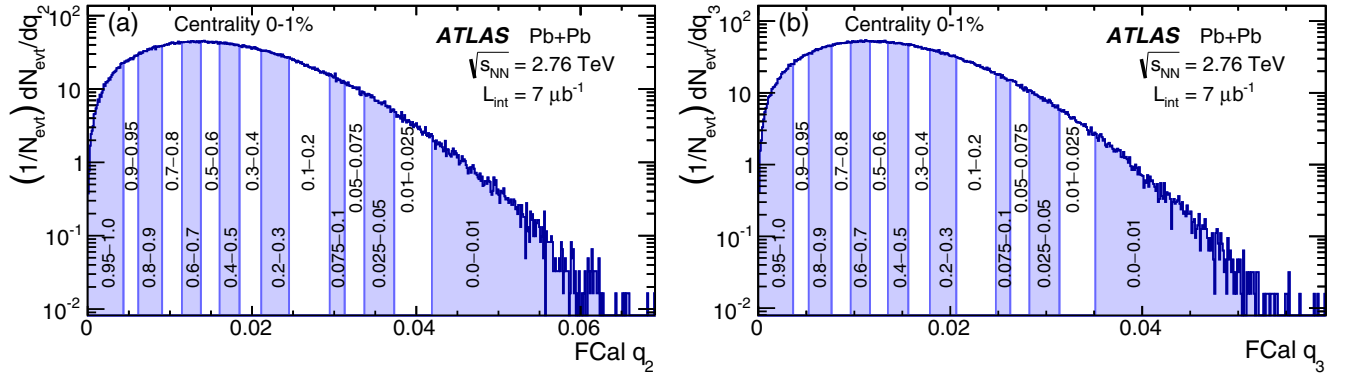
FIG. 1. (Color online) The distributions of the magnitude of the flow vector, q_2 (left) and q_3 (right), calculated in the FCal via Eq. (7) in the 1% most central collisions. The vertical lines indicate the boundaries of the 15 q_m ranges, each containing a fraction of events as indicated.

first q_m interval in the five centrality intervals, 0%–1%, 1%–2%, . . . , 4%–5%. The default analysis uses 15 nonoverlapping q_m intervals defined in Fig. 1. For better statistical precision, sometimes they are regrouped into wider q_m intervals.

B. Two-particle correlations

The two-particle correlation analysis closely follows a previous ATLAS publication [11], where it is described in detail, so the analysis is only briefly summarized here. For a given event class, the two-particle correlation is measured as a function of relative azimuthal angle $\Delta\phi = \phi_a - \phi_b$ and relative pseudorapidity $\Delta\eta = \eta_a - \eta_b$. The labels a and b denote the two particles in the pair, which may be selected from different p_T intervals. The two-particle correlation function is constructed as the ratio of distributions for same-event pairs [or foreground pairs $S(\Delta\phi, \Delta\eta)$] and mixed-event pairs [or background pairs $B(\Delta\phi, \Delta\eta)$]:

$$C(\Delta\phi, \Delta\eta) = \frac{S(\Delta\phi, \Delta\eta)}{B(\Delta\phi, \Delta\eta)}. \quad (9)$$

The mixed-event pair distribution is constructed from track pairs from two separate events with similar centrality and z_{vtx}, such that it properly accounts for detector inefficiencies and nonuniformity, but contains no physical correlations. Charged particles measured by the ID with a pair acceptance extending up to $|\Delta\eta| = 5$ are used for constructing the correlation function.

This analysis focuses mainly on the shape of the correlation function in $\Delta\phi$. A set of one-dimensional (1D) $\Delta\phi$ correlation functions is built from the ratio of the foreground distributions to the background distributions, both projected onto $\Delta\phi$:

$$C(\Delta\phi) = \frac{\int S(\Delta\phi, \Delta\eta) d\Delta\eta}{\int B(\Delta\phi, \Delta\eta) d\Delta\eta}. \quad (10)$$

The normalization is fixed by scaling the number of the mixed-event pairs to be the same as the number of same-event pairs for $2 < |\Delta\eta| < 5$, which is then applied to all $\Delta\eta$ slices.

Figure 2 shows the 1D correlation functions for $2 < |\Delta\eta| < 5$ calculated in the low-p_T region ($0.5 < p_T^{a,b} < 2$ GeV) in the
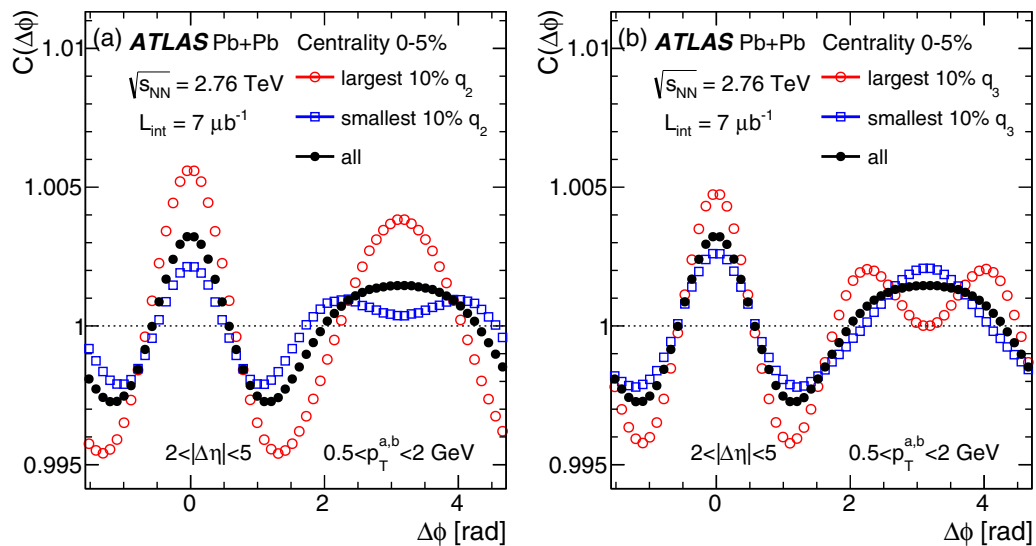

FIG. 2. (Color online) The correlation functions $C(\Delta\phi)$ for pairs with $|\Delta\eta| > 2$ and $0.5 < p_T < 2$ GeV in 0%–5% centrality. The correlation functions for events with the largest 10% and smallest 10% q_m values are also shown for $m = 2$ (left) and $m = 3$ (right). The statistical uncertainties are smaller than the symbols.

0%–5% most central collisions. The correlation functions are also shown for events selected with the largest and smallest q_2 values (left panel) or q_3 values (right panel). The magnitude of the modulation correlates strongly with the q_m value, reflecting the fact that the global ellipticity or triangularity can be selected by q_2 or q_3 in the forward rapidity interval. The correlation function for events with smallest q_2 or largest q_3 values shows a double-peak structure on the away side ($\Delta\phi \sim \pi$). This structure reflects the dominant contribution of the triangular flow under these q_m selections. Similar double-peak structures are also observed in ultracentral Pb + Pb collisions without event-shape selection [11,42].

The 1D correlation function in $\Delta\phi$ is then expressed as a Fourier series:

$$C(\Delta\phi) = \frac{\int C(\Delta\phi)d\Delta\phi}{2\pi}\left[1 + 2\sum_n v_{n,n}\cos(n\Delta\phi)\right]. \quad (11)$$

The Fourier coefficients are calculated directly from the correlation function as $v_{n,n} = \langle\cos(n\Delta\phi)\rangle$. The single-particle azimuthal anisotropy coefficients v_n are obtained via the factorization relation commonly used for collective flow in heavy-ion collisions [11,12,43,44]:

$$v_{n,n}\left(p_T^a, p_T^b\right) = v_n\left(p_T^a\right)v_n\left(p_T^b\right). \quad (12)$$

From Eq. (12), v_n is calculated as

$$v_n(p_T) = v_{n,n}\left(p_T, p_T^b\right)\Big/\sqrt{v_{n,n}\left(p_T^b, p_T^b\right)}, \quad (13)$$

where p_T^a is simply denoted by p_T from now on, and the default transverse momentum range for p_T^b is chosen to be $0.5 < p_T^b < 2$ GeV, where the hydrodynamic viscous corrections are not too large. The v_n values obtained using this method measure, in effect, the root-mean-square (r.m.s.) values of the event-by-event v_n [43]. A detailed test of the factorization behavior was carried out [11,12] by comparing the $v_n(p_T)$ obtained for different p_T^b ranges, and factorization was found to hold to within 10% for $p_T^b < 4$ GeV for the centrality ranges studied in this paper.

C. Systematic uncertainties

Other than the classification of events according to q_m ($m = 2$ or 3), the analysis procedure is nearly identical to the previous ATLAS measurement [11] based on the same data set. Most systematic uncertainties are the same, and they are summarized here.

The correlation function relies on the pair acceptance function to reproduce and cancel the detector acceptance effects in the foreground distribution. A natural way of quantifying the influence of detector effects on $v_{n,n}$ and v_n is to express the single-particle and pair acceptance functions as Fourier series [as in Eq. (11)] and measure the coefficients v_n^{det} and $v_{n,n}^{\mathrm{det}}$. The resulting coefficients for pair acceptance, $v_{n,n}^{\mathrm{det}}$, are the product of two single-particle acceptances, $v_n^{\mathrm{det,a}}$ and $v_n^{\mathrm{det,b}}$. In general, the pair acceptance function in $\Delta\phi$ is quite flat: The maximum variation from its average is observed to be less than 0.001, and the corresponding $|v_{n,n}^{\mathrm{det}}|$ values are found to be less than 1.5×10^{-4}. These $v_{n,n}^{\mathrm{det}}$ effects are expected to cancel to a large extent in the correlation function, and only a small fraction contributes to the uncertainties in the pair acceptance function. Three possible residual effects for $v_{n,n}^{\mathrm{det}}$ are studied in Ref. [11]: (1) the time dependence of the pair acceptance, (2) the effect of imperfect centrality matching, and (3) the effect of imperfect z_{vtx} matching. In each case, the residual $v_{n,n}^{\mathrm{det}}$ values are evaluated by a Fourier expansion of the ratio of the pair acceptances before and after the variation. The systematic uncertainty of the pair acceptance is the sum in quadrature of these three estimates, which is $\delta v_{n,n} < 5 \times 10^{-6}$ for $2 < |\Delta\eta| < 5$. This absolute uncertainty is propagated to the uncertainty in v_n, and it is the dominant uncertainty when v_n is small, e.g., for v_5 in central collisions. This uncertainty is found to be uncorrelated with the q_m selection, and hence it is assumed not to cancel between different q_m intervals.

A further type of systematic uncertainty includes the sensitivity of the analysis to track selection requirements and track reconstruction efficiency, variation of v_n between different running periods, and trigger and event selection. The effect of the track reconstruction efficiency was evaluated in Ref. [13]; the other effects were evaluated in Ref. [11]. Most systematic uncertainties cancel in the correlation function when dividing the foreground distribution by the background distribution. The estimated residual effects are summarized in Table II. Most of these uncertainties are expected to be correlated between different q_m intervals.

Finally, owing to the anisotropy of particle emission, the detector occupancy is expected to be larger in the direction of the EP, where the particle density is larger. Any occupancy effects depending on azimuthal angle may lead to a small angle-dependent efficiency variation, which may slightly reduce the measured v_n coefficients. The magnitude of such an occupancy-dependent variation in tracking efficiency is evaluated using the HIJING simulation with flow imposed on

TABLE II. Relative systematic uncertainties on the measured v_n owing to track selection requirements, track reconstruction efficiency, variation between different running periods, trigger selection, consistency between true and reconstructed v_n in HIJING simulation, and the quadrature sum of individual terms. Most of these uncertainties are correlated between different ranges of q_m ($m = 2$ or 3).

	v_2	v_3	v_4	v_5	q_m dependent
Track selection (%)	0.3	0.3	1.0	2.0	Yes
Track reconstruction efficiency (%)	0.1–1.0	0.2–1.5	0.2–2.0	0.3–2.5	Yes
Running periods (%)	0.3–1.0	0.7–2.1	1.2–3.1	2.3	No
Trigger (%)	0.5–1.0	0.5–1.0	0.5–1	1.0	Yes
MC closure and occupancy effects (%)	1.0	1.5	2.0	3.5	Yes
Sum of above (%)	1.2–2.0	1.8–3.2	2.6–4.4	4.7–5.4	

the generated particles [13]. The reconstructed v_n values are compared to the generated v_n signal. The differences are taken as an estimate of the systematic uncertainties. These differences are found to be a few percent or less and are included in Table II. Because this effect is proportional to the flow signal, it is expected to partially cancel between different q_m ranges.

V. RESULTS

A. Fourier coefficients v_n and their correlations with q_m

Figure 3 shows the $v_n(p_T)$ for $n = 2$ to 5 extracted via Eq. (13) for events in the 20%–30% centrality interval. The results show nontrivial correlations with both the q_2 (left column) or q_3 (right column) selections. In the case of the q_2 selection, the v_2 values are largest for events selected with the largest q_2 and smallest for events selected with the smallest q_2, with a total change of more than a factor of two. A similar dependence on q_2 is also seen for $v_4(p_T)$ and $v_5(p_T)$ (two bottom panels). In contrast, the extracted $v_3(p_T)$ values are anticorrelated with q_2; the overall change in $v_3(p_T)$ is also significantly smaller ($<20\%$ across the q_2 range). In the case of the q_3 selection, a strong positive correlation is observed for v_3 and v_5, and a weak anticorrelation is observed for v_2 and v_4. All these correlations are observed to be nearly independent of p_T, suggesting that the response of v_n to the change in the event shape is largely independent of p_T. As a consistency check, the inclusive results without q_m selection are compared with previously published results from Ref. [11]: The differences are less than 0.6% for v_2 and increase to 2%–3% for higher harmonics, which are well within the systematic uncertainties quoted in Table II.

Figure 4 shows the correlation between v_n and q_m for $m = 2$ (left column) and $m = 3$ (right column) in several centrality intervals in a low p_T range ($0.5 < p_T < 2$ GeV). Because the v_n-q_m correlation depends only weakly on p_T, this plot captures the essential features of the correlation between v_n and q_m shown in Fig. 3. Owing to the finite number of particles in an event, the measured q_m values fluctuate relative to the true values, diluting the correlations with v_n. The influence of smearing on the q_2 is much smaller than that for the q_3 simply because the v_2 signal is much bigger than the v_3 signal. However, because both the v_m-q_m and the v_n-q_m correlations are measured, the results are presented directly as v_m-v_n correlations for various q_m selections. The level of detail contained in the v_m-v_n correlation is controlled by the dynamic range of v_m when varying the q_m selection. This dynamic range depends strongly on event centrality. For example, in the 10%–15% centrality interval, v_2 is varied by a factor of 3.1 by selecting on q_2 and v_3 is varied by a factor of 2.4 by selecting on q_3. In the 40%–45% centrality interval, however, owing to stronger statistical smearing of q_m, the v_2 and v_3 are only varied by a factor of 2.7 and 1.7, respectively. Hence, the event-shape selection is precise in central and midcentral collisions and is expected to be less precise in peripheral collisions.

In general, correlations v_m-q_m and v_n-q_m can be measured in different p_T ranges, and the derived v_m-v_n correlation can be categorized into three types: (1) the correlation between v_m in two different p_T ranges, $v_m\{p_T^a\}$-$v_m\{p_T^b\}$, (2) the correlation between v_m and another flow harmonic of different order v_n in the same p_T range, $v_m\{p_T\}$-$v_n\{p_T\}$, and (3) the correlation between

v_m and v_n in different p_T ranges, $v_m\{p_T^a\}$-$v_n\{p_T^b\}$. However, the $v_m\{p_T^a\}$-$v_n\{p_T^b\}$ correlation can be obtained by combining two correlations, $v_m\{p_T^a\}$-$v_m\{p_T^b\}$ and $v_m\{p_T^b\}$-$v_n\{p_T^b\}$, so it does not carry independent information. This paper, therefore, focuses on the first two types of correlation.

The results for v_m-v_n correlations are organized as follows. Section V B presents correlations of v_2 or v_3 between two different p_T ranges. The v_2-v_3 correlations are discussed in Sec. V C. This is followed by v_2-v_4 and v_3-v_4 correlations in Sec. V D and v_2-v_5 and v_3-v_5 correlations in Sec. V E, where a detailed analysis is performed to separate the linear and nonlinear components of v_4 and v_5. The eccentricity scaling behavior of the extracted linear component of v_n is presented in Sec. V F.

B. Correlation of v_2 or v_3 between two different p_T ranges

Figure 5 shows the correlation of v_m for $m = 2$ (left panel) or $m = 3$ (right panel) between two p_T ranges for various centrality intervals. The x axis represents v_m values in the $0.5 < p_T < 2$ GeV range, while the y axis represents v_m values from a higher range of $3 < p_T < 4$ GeV. Each data point corresponds to a 5% centrality interval within the overall centrality range of 0%–70%. Going from central collisions (left end of the data points) to the peripheral collisions (right end of the data points), v_m first increases and then decreases along both axes, reflecting the characteristic centrality dependence of v_m, well known from previous flow analyses [10,11]. The rate of decrease is larger at higher p_T, resulting in a "boomeranglike" structure in the correlation. The stronger centrality dependence of v_m at higher p_T is consistent with larger viscous-damping effects expected from hydrodynamic calculations [45].

In the next step, events in each centrality interval are further divided into q_m intervals, as described in Sec. IV A. With this further subdivision, each data point in Fig. 5 turns into a group of data points, which may follow a different correlation pattern. These data points are shown in Fig. 6 (markers) overlaid with the overall centrality dependence prior to the event-shape selection from Fig. 5 (the "boomerang"). For clarity, the results are shown only for seven selected centrality intervals. Unlike the centrality dependence, the v_m correlation within a given centrality interval approximately follows a straight line passing very close to the origin. The small nonzero intercepts can be attributed to a residual centrality dependence of the v_m-v_m correlation within the finite centrality intervals used. This approximately linear correlation suggests that, once the event centrality or the overall event multiplicity is fixed, the viscous-damping effects on v_m change very little with the variation of the event shape via q_m selection. The influence of viscosity on flow harmonics is mainly controlled by the event centrality (or the overall system size).

C. v_2-v_3 correlation

Figure 7(a) shows the centrality dependence of the correlation between v_2 and v_3 measured in $0.5 < p_T < 2$ GeV. The boomeranglike structure in this case reflects mostly the fact that v_3 has a much weaker centrality dependence than v_2 [11]. Figure 7(b) overlays the centrality dependence of the v_2-v_3 correlation (thick solid line) with those obtained for
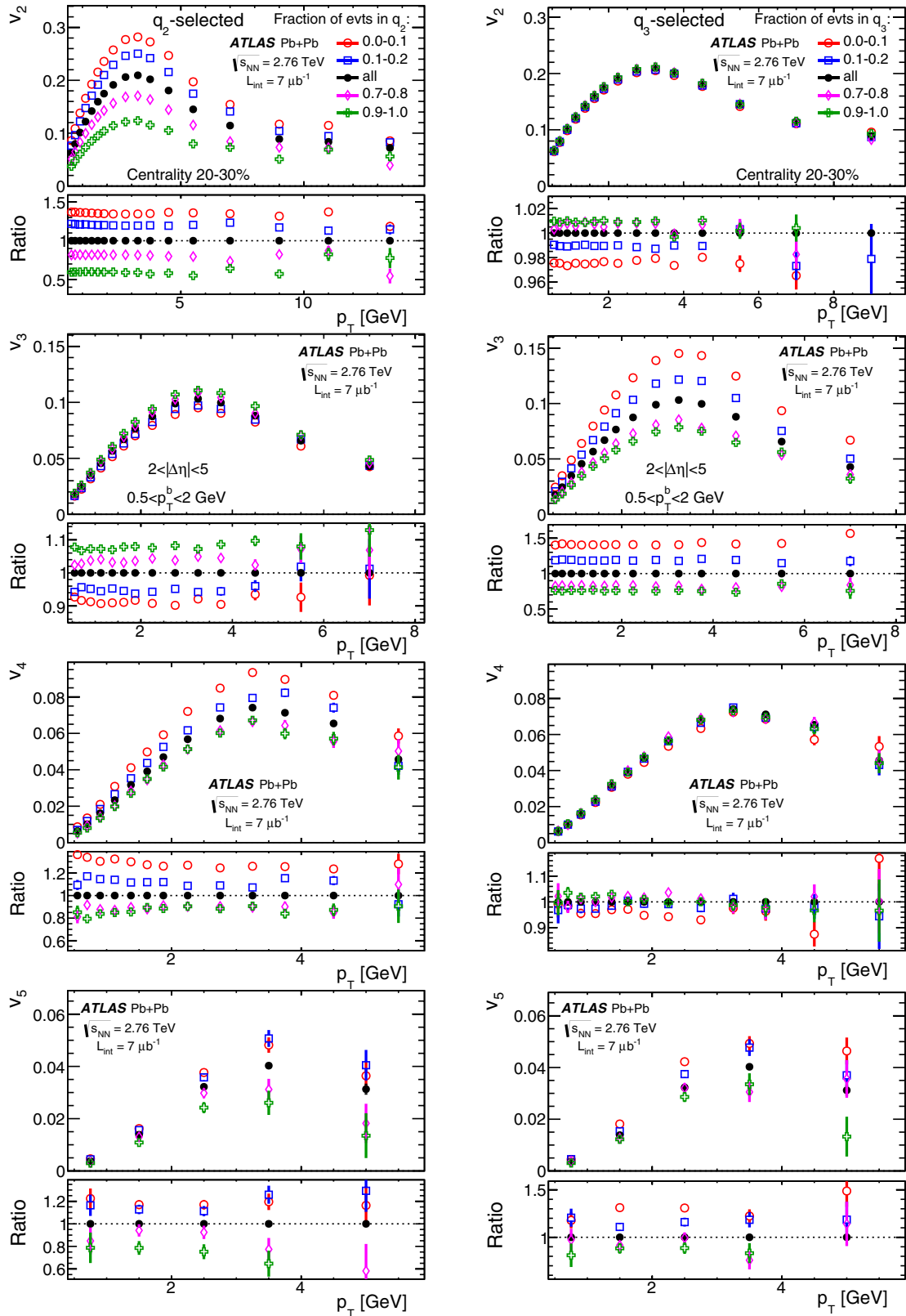
FIG. 3. (Color online) The harmonic flow coefficients $v_n(p_T)$ in the 20%–30% centrality interval for events selected on either q_2 (left column) or q_3 (right column) for $n = 2$ (top row), $n = 3$ (second row), $n = 4$ (third row), and $n = 5$ (bottom row). They are calculated for reference p_T of $0.5 < p_T^b < 2$ GeV [Eq. (13)]. The top part of each panel shows the $v_n(p_T)$ for events in the 0–0.1, 0.1–0.2, 0.7–0.8, and 0.9–1 fractional ranges of q_m (open symbols), as well as for inclusive events without q_m selection (solid symbols). The bottom part of each panel shows the ratios of the $v_n(p_T)$ for q_m-selected events to those obtained for all events. Only statistical uncertainties are shown.
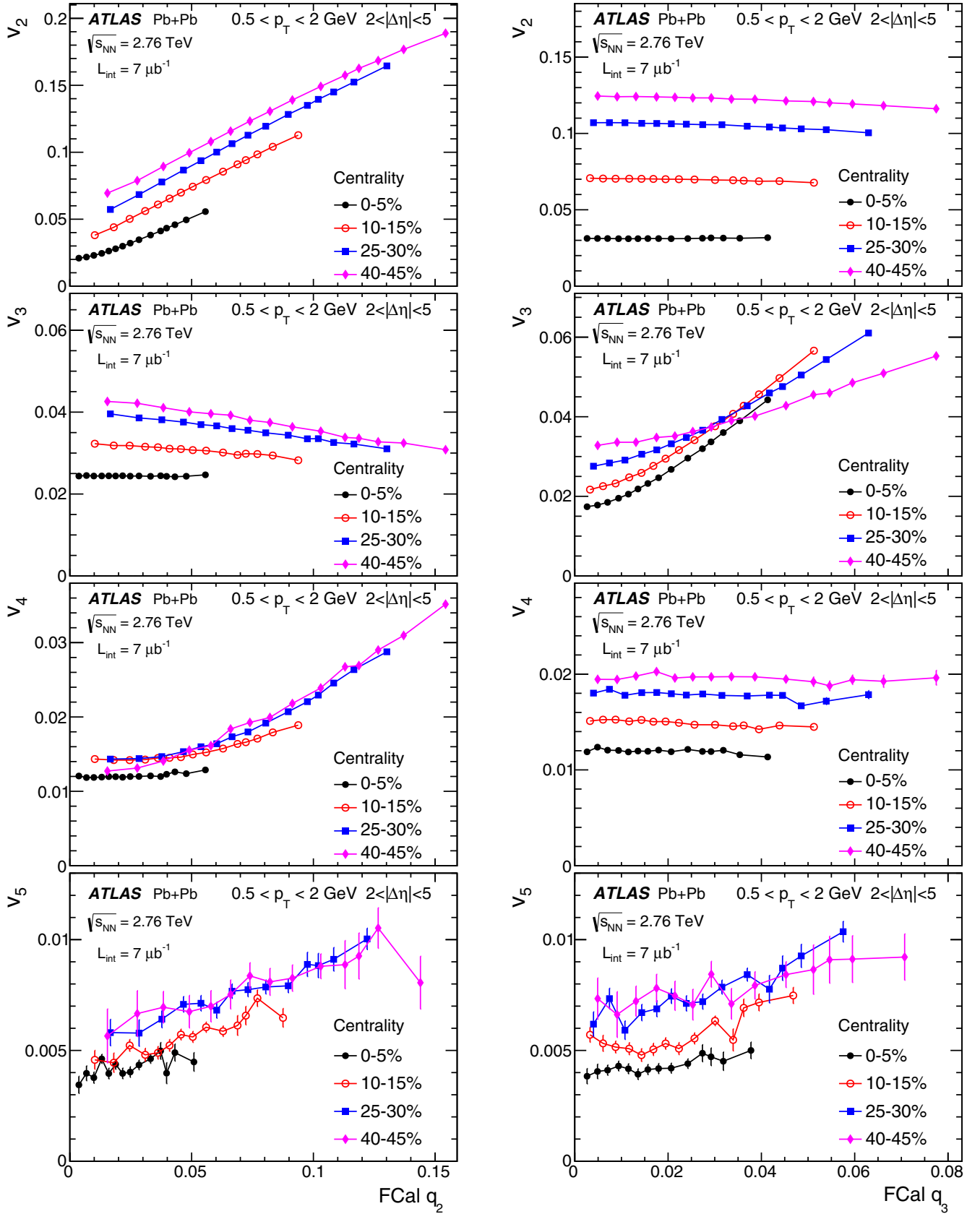
FIG. 4. (Color online) The correlations between v_n and q_2 (left column) and q_3 (right column) in four centrality intervals with $n = 2$ (top row), $n = 3$ (second row), $n = 4$ (third row), and $n = 5$ (bottom row), where v_n is calculated in $0.5 < p_T < 2$ GeV. Only statistical uncertainties are shown. The lines connecting data points are for guidance only.
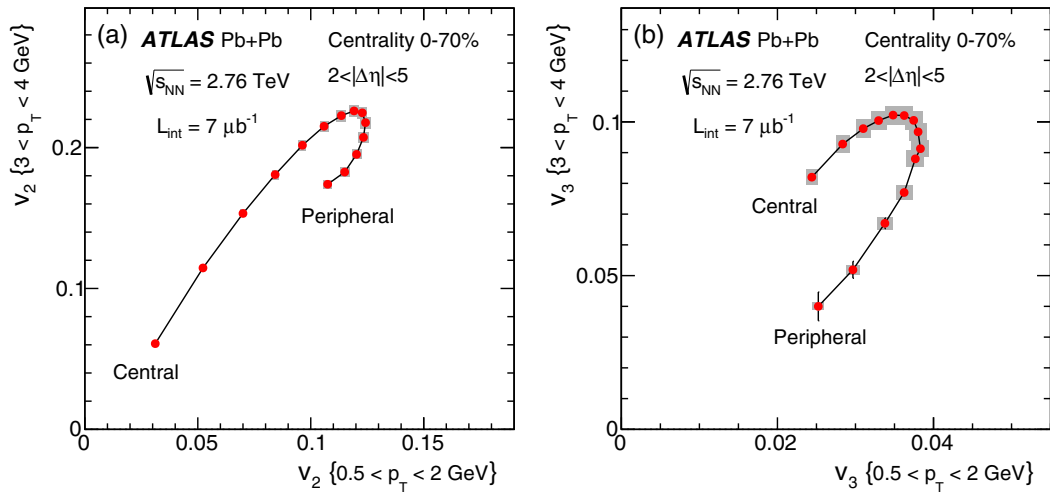
FIG. 5. (Color online) The correlation of the v_m between $0.5 < p_T < 2$ GeV (x axis) and $3 < p_T < 4$ GeV (y axis) for $m = 2$ (left) and $m = 3$ (right). The v_m values are calculated for fourteen 5% centrality intervals in the centrality range 0%–70% without event-shape selection. The data points are connected to show the boomerang trend from central to peripheral collisions, as indicated. The error bars and shaded boxes represent the statistical and systematic uncertainties, respectively. These uncertainties are often smaller than the symbol size.

different q_2 event classes (markers). The correlation within a fixed centrality interval follows a path very different from the centrality dependence: The v_2 and v_3 are always anticorrelated with each other within a given centrality, whereas they are positively correlated as a function of centrality. Because the v_2 and v_3 are driven by the initial eccentricities, $v_2 \propto \epsilon_2$ and $v_3 \propto \epsilon_3$, one may expect similar anticorrelation between ϵ_2 and ϵ_3. Indeed, a calculation based on a multiphase transport model [46] shows that such anticorrelations exist in the initial geometry and they are transferred into similar anticorrelations between v_2 and v_3 by the collective expansion [28].

To illustrate this anticorrelation more clearly, the v_2-v_3 correlation data are replotted in Fig. 8, separately for each centrality. The data are compared with the ϵ_2-ϵ_3 correlations calculated via Eq. (2) from the MC Glauber model [34] and the MC-KLN model [47]. The MC-KLN model is based on the MC Glauber model, but takes into account gluon saturation effects in the initial geometry. One hundred million events were generated for each model and grouped into centrality intervals according to the impact parameter. The r.m.s. ϵ_n value for each centrality interval is rescaled by a factor s_n to match the inclusive v_n value, which effectively is also the r.m.s. value of
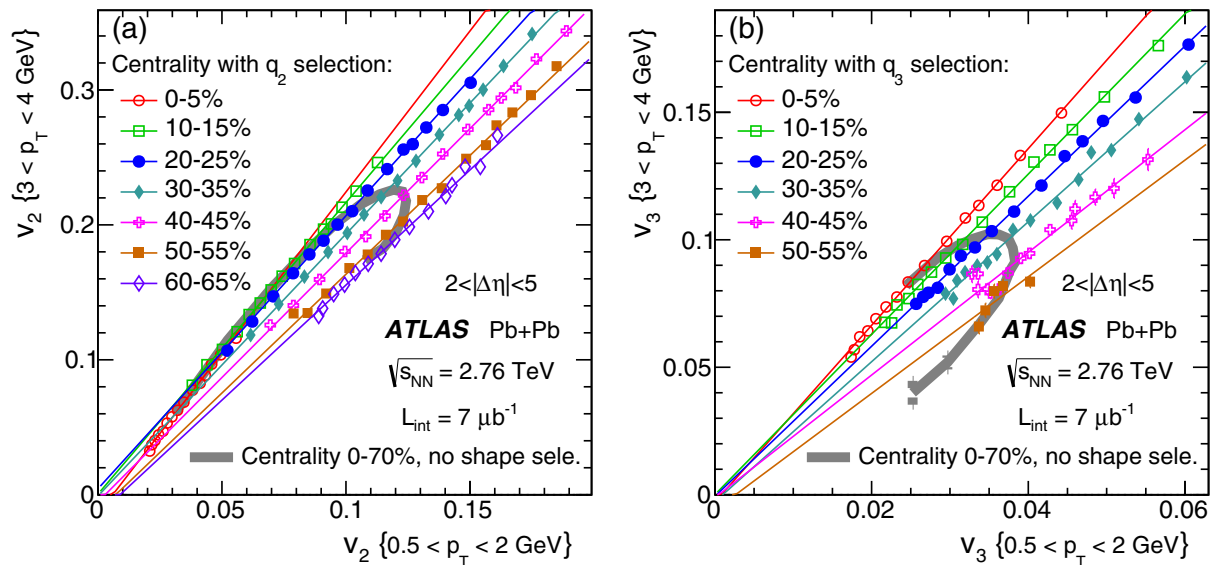

FIG. 6. (Color online) The correlation of v_m between the $0.5 < p_T < 2$ GeV (x axis) and $3 < p_T < 4$ GeV range (y axis) for $m = 2$ (left) and $m = 3$ (right) in various centrality intervals. The data points are calculated in various q_m intervals defined in Fig. 1 for each centrality, and they increase monotonically with increasing q_m value. These data are overlaid with the centrality dependence without q_m selection from Fig. 5. The thin solid straight lines represent a linear fit of the data in each centrality interval, and error bars represent the statistical uncertainties.
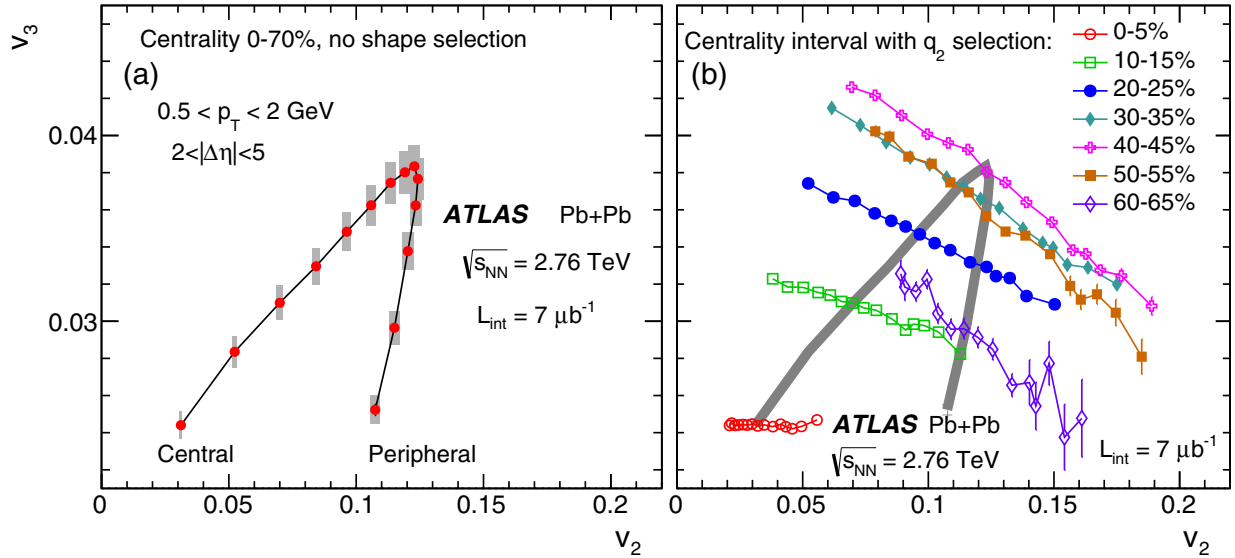
FIG. 7. (Color online) The correlation of v_2 (x axis) with v_3 (y axis) both measured in $0.5 < p_T < 2$ GeV. The left panel shows the v_2 and v_3 values for fourteen 5% centrality intervals over the centrality range 0%–70% without event-shape selection. The data points are connected to show the boomerang trend from central to peripheral collisions, as indicated. The right panel shows the v_2 and v_3 values in the 15 q_2 intervals in seven centrality ranges (markers) with larger v_2 value corresponding to larger q_2 value; they are overlaid with the centrality dependence from the left panel. The error bars and shaded boxes represent the statistical and systematic uncertainties, respectively.

v_n [see Eq. (13)]:

$$s_n = \frac{v_n}{\sqrt{\langle \epsilon_n^2 \rangle}}. \qquad (14)$$

The parameter s_n changes with centrality but is assumed to be a constant within a given centrality interval. These constants are then used to rescale the ϵ_2-ϵ_3 correlation to be compared with the v_2-v_3 correlation in each centrality interval, as shown in Fig. 8. In most centrality intervals the rescaled ϵ_2-ϵ_3 correlation shows very good agreement with the v_2-v_3 correlation seen in the data. However, significant deviations are observed in more central collisions (0%–20% centrality range). Therefore, the v_2-v_3 correlation data presented in this analysis can provide valuable constraints for further tuning of the initial-geometry models. The v_2-v_3 correlations in Fig. 8 are parametrized by a linear function,

$$v_3 = k v_2 + v_3^0, \qquad (15)$$

where the intercept v_3^0 provides an estimate of the asymptotic v_3 value for events that have zero v_2 for each centrality. The fit parameters are summarized as a function of centrality ($N_{\rm part}$) in the last two panels of Fig. 8.

D. v_2-v_4 and v_3-v_4 correlations

Figure 9(a) shows the correlation between v_2 and v_4 in $0.5 < p_T < 2$ GeV prior to the event-shape selection. The boomeranglike structure is less pronounced than that for the v_2-v_3 correlation shown in Fig. 7(a). Figure 9(b) shows the v_2-v_4 correlation for different q_2 event classes (markers) overlaid with the centrality dependence taken from Fig. 9(a) (thick solid line). The correlation within a given centrality interval is broadly similar to the trend of the correlation without event-shape selection, but without any boomerang

effect. Instead, the shape of the correlation exhibits a nonlinear rise for large v_2 values.

To understand further the role of the linear and nonlinear contributions to v_4, the v_2-v_4 correlation data in Fig. 9 are shown again in Fig. 10, separately for each centrality. The data are compared with the ϵ_2-ϵ_4 correlation rescaled according to Eq. (14). The rescaled ϵ_2-ϵ_4 correlations fail to describe the data, suggesting that the linear component alone associated with ϵ_4 in Eq. (5) is not sufficient to explain the measured v_2-v_4 correlation.

To separate the linear and nonlinear components in the v_2-v_4 correlation, the data are fitted to the following functional form:

$$v_4 = \sqrt{c_0^2 + \left(c_1 v_2^2\right)^2}. \qquad (16)$$

This function is derived from Eq. (5), by ignoring the higher-order nonlinear terms (those in "$\cdots$") and a possible cross term that is proportional to $\langle \cos 4(\Psi_2 - \Psi_4) \rangle$. The fits, which are shown in Fig. 10, describe the data well for all centrality intervals. The excellent description of the data by the fits suggests that either the contributions from higher-order nonlinear terms and $\langle \cos 4(\Psi_2 - \Psi_4) \rangle$ are small or the cross-term is, in effect, included in the nonlinear component of the fits. The centrality ($N_{\rm part}$) dependence of the fit parameters is shown in the last two panels of Fig. 10.

The c_0 term from the fits can be used to decompose v_4, without q_2 selection, into linear and nonlinear terms for each centrality interval as

$$v_4^L = c_0, \quad v_4^{\rm NL} = \sqrt{v_4^2 - c_0^2}. \qquad (17)$$

The results as a function of centrality are shown in Fig. 11 (open circles and squares). The linear term associated with ϵ_4 depends only weakly on centrality and becomes the dominant part of v_4 for $N_{\rm part} > 150$, or 0%–30% centrality
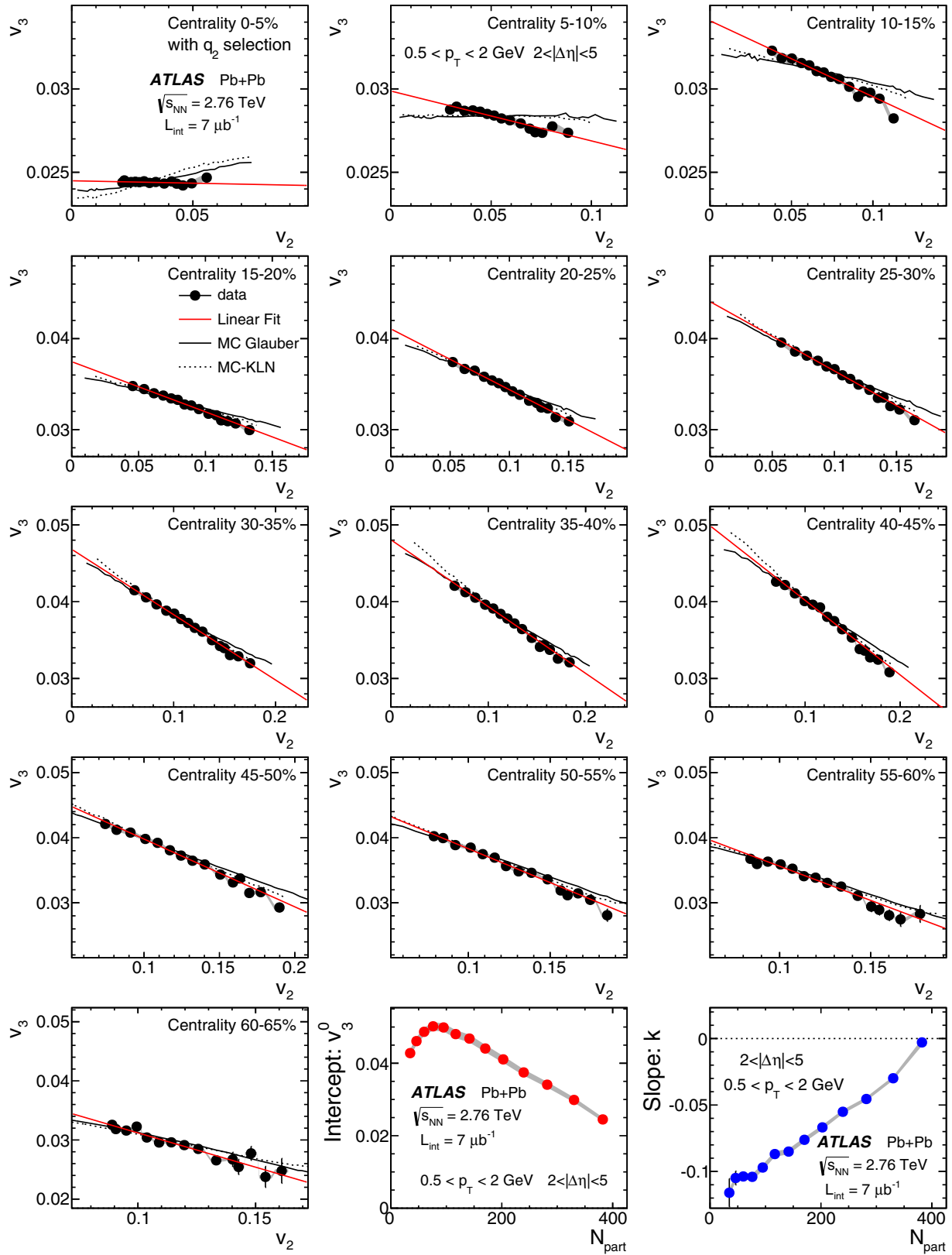
FIG. 8. (Color online) The correlation of v_2 (x axis) with v_3 (y axis) in $0.5 < p_T < 2$ GeV for 15 q_2 selections in thirteen 5% centrality intervals. The data are compared with the rescaled ϵ_2-ϵ_3 correlation from MC Glauber and MC-KLN models in the same centrality interval. The data are also parametrized with a linear function [Eq. (15)], taking into account both the statistical and the systematic uncertainties. The N_{part} dependence of the fit parameters is shown in the last two panels. The error bars and shaded bands represent the statistical and systematic uncertainties, respectively.
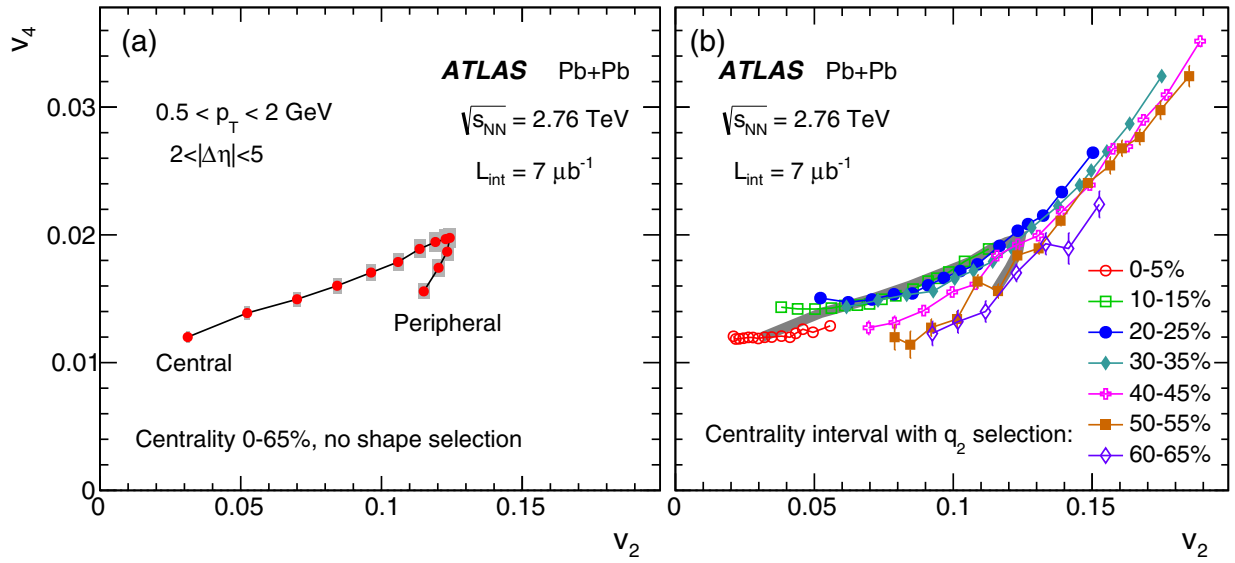
FIG. 9. (Color online) The correlation of v_2 (x axis) with v_4 (y axis) both measured in $0.5 < p_T < 2$ GeV. The left panel shows the v_2 and v_4 values for thirteen 5% centrality intervals over the centrality range 0%–65% without event-shape selection. The data points are connected to show the boomerang trend from central to peripheral collisions, as indicated. The right panel shows the v_2 and v_4 values in different q_2 intervals in seven centrality ranges (markers) with larger v_2 value corresponding to larger q_2 value; they are overlaid with the centrality dependence from the left panel. The error bars and shaded boxes represent the statistical and systematic uncertainties, respectively.

range. The nonlinear term increases as the collisions become more peripheral and becomes the dominant part of v_4 for $N_{part} < 120$.

Because the contributions of higher-order nonlinear terms are small, as suggested by the fits discussed above, the linear and nonlinear contributions can also be estimated directly from the previously published EP correlator $\langle\cos 4(\Phi_2 - \Phi_4)\rangle$ from ATLAS [14]:

$$v_4^{NL,EP} = v_4\langle\cos 4(\Phi_2 - \Phi_4)\rangle, \quad v_4^{L,EP} = \sqrt{v_4^2 - (v_4^{NL,EP})^2}.$$
(18)

Results for this decomposition are shown in Fig. 11 (the hashed bands labeled EP), and they agree with the result obtained from the present analysis.

Figure 12(a) shows the correlation between v_3 and v_4 in $0.5 < p_T < 2$ GeV prior to the event-shape selection. The data fall nearly on a single curve, reflecting the similar centrality dependence trends for v_3 and v_4 [11]. Figure 12(b) shows the v_3-v_4 correlation for different q_3 event classes (colored symbols) overlaid with the centrality dependence taken from Fig. 12(a) (thick solid line). A slight anticorrelation between v_3 and v_4 is observed, which is consistent with the fact that v_4 has a large nonlinear contribution from v_2 (Fig. 11), which, in turn, is anticorrelated with v_3 (Fig. 7).

E. v_2-v_5 and v_3-v_5 correlations

The analysis of v_2-v_5 and v_3-v_5 correlations proceeds in the same manner as for the v_2-v_4 and v_3-v_4 correlations. A separation of the linear and nonlinear components of v_5 is made.

Figure 13 shows the v_2-v_5 correlation in $0.5 < p_T < 2$ GeV with q_2 selection, separately for each centrality interval.

The data are compared with the ϵ_2-ϵ_5 correlations rescaled according to Eq. (14). The rescaled ϵ_2-ϵ_5 correlations fail to describe the data in all centrality intervals, suggesting that the nonlinear contribution in Eq. (6) is important. To separate the linear and nonlinear component in the v_2-v_5 correlation, the data are fitted with the function

$$v_5 = \sqrt{c_0^2 + (c_1 v_2 v_3)^2},$$
(19)

where the higher-order nonlinear terms in Eq. (6) and a possible cross-term associated with $\langle\cos(2\Psi_2 + 3\Psi_3 - 5\Psi_5)\rangle$ are dropped. For each centrality interval, Eq. (15) is used to fix the v_3 value for each v_2 value. The fits are shown in Fig. 13 and describe the data well for all centrality intervals. The centrality (N_{part}) dependence of the fit parameters is shown in the last two panels of Fig. 13. The c_0 represents an estimate of the linear component of v_5, and the nonlinear term is driven by c_1, which has a value of $\sim$1.5–2.

Figure 14 shows the v_3-v_5 correlations with q_3 selection in various centrality intervals. If Eq. (19) is a valid decomposition of v_5, then it should also describe these correlations. Figure 14 shows that this indeed is the case. The parameters extracted from a fit to Eq. (19), as shown in the last two panels of Fig. 14, are consistent with those obtained from v_2-v_5 correlations.

From the fit results in Figs. 13 and 14, the inclusive v_5 values prior to event-shape selection are decomposed into linear and nonlinear terms for each centrality interval as

$$v_5^L = c_0, \quad v_5^{NL} = \sqrt{v_5^2 - c_0^2}.$$
(20)

The results as a function of centrality are shown in the two panels of Fig. 15, corresponding to Figs. 13 and 14, respectively. Results for the two decompositions show consistent centrality dependence: The linear term associated with ϵ_5 dominates
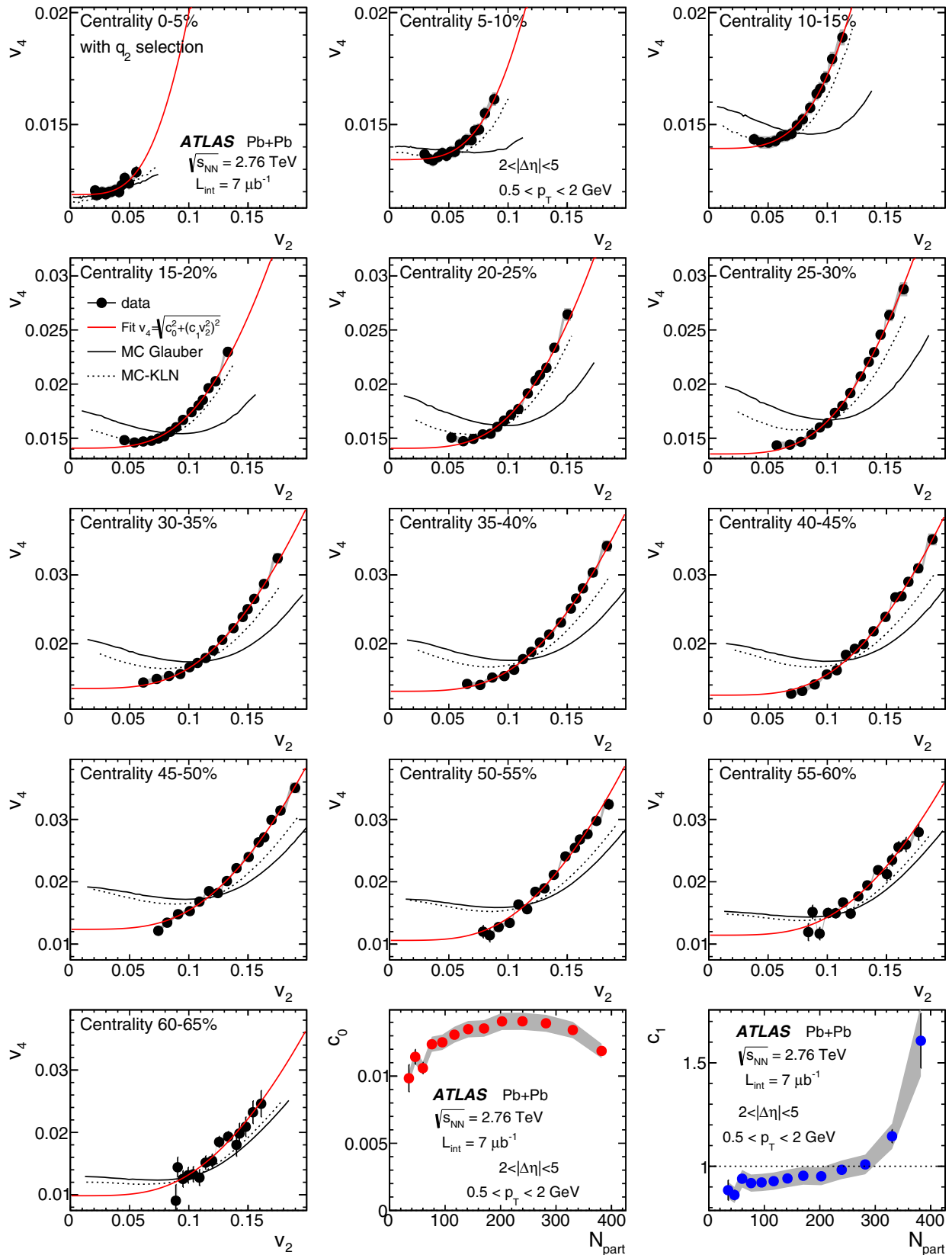
FIG. 10. (Color online) The correlation of v_2 (x axis) with v_4 (y axis) in $0.5 < p_T < 2$ GeV for 15 q_2 selections in thirteen 5% centrality intervals. The data are compared with the rescaled ϵ_2-ϵ_4 correlation from MC Glauber and MC-KLN models in the same centrality interval. The data are also parametrized with Eq. (16), taking into account both statistical and systematic uncertainties. The N_{part} dependence of the fit parameters is shown in the last two panels. The error bars and shaded bands represent the statistical and systematic uncertainties, respectively.
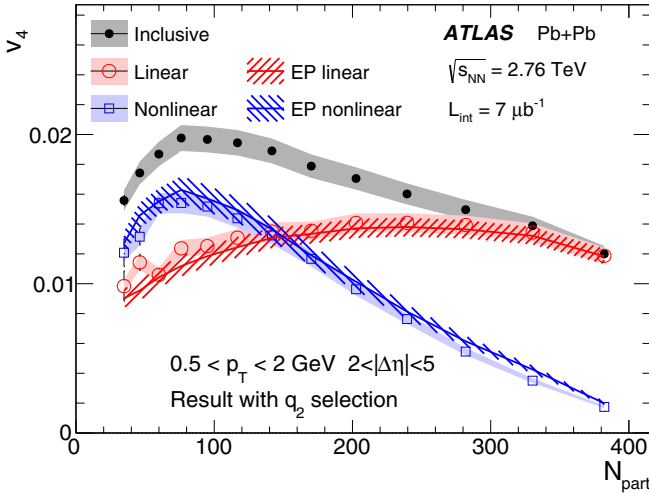
FIG. 11. (Color online) The centrality (N_{part}) dependence of the v_4 in $0.5 < p_T < 2$ GeV and the associated linear and nonlinear components extracted from the fits in Fig. 10 and Eq. (17). They are compared with the linear and nonlinear component estimated from the previously published EP correlations [14] via Eq. (18). The error bars represent the statistical uncertainties, while the shaded bands or hashed bands represent the systematic uncertainties.

the v_5 signal only in the most central collisions ($N_{part} > 300$ or 0%–10% centrality). The nonlinear term increases as the collisions become more peripheral and becomes the dominant part of v_5 for $N_{part} \lesssim 280$.

Similar to the case of v_2-v_4 correlation, the linear and non-linear contribution to v_5 can also be estimated directly from the previously published EP correlator $\langle \cos(2\Phi_2 + 3\Phi_3 - 5\Phi_5) \rangle$

from ATLAS [14]:

$$v_5^{NL,EP} = v_5 \langle \cos(2\Phi_2 + 3\Phi_3 - 5\Phi_5) \rangle,$$
$$v_5^{L,EP} = \sqrt{v_5^2 - (v_5^{NL,EP})^2}. \quad (21)$$

Results for this decomposition are shown as solid curves in Fig. 15, and they agree well with the result obtained in the present analysis.

F. Eccentricity-scaled v_n

One quantity often used to characterize the collective response of the medium to the initial geometry is the response coefficient k_n defined in Eq. (4). Because the v_n obtained from the two-particle correlation method effectively measure the r.m.s. values of the event-by-event v_n [43], a more appropriate quantity to characterize the collective response is the ratio of v_n to the r.m.s. eccentricity [22,24]: $v_n/\sqrt{\langle \epsilon_n^2 \rangle}$. This quantity can be directly calculated for v_2 and v_3 because they are mostly driven by ϵ_2 and ϵ_3. However, for higher-order flow harmonics, it is more appropriate to use the extracted linear component v_n^L to make the ratios as it is more directly related to the ϵ_n. The v_n^L is taken as the c_0 term obtained from the two-component fits in Fig. 10 for $n = 4$ and Fig. 13 for $n = 5$. Figure 16 shows the centrality dependence of $v_n/\sqrt{\langle \epsilon_n^2 \rangle}$ for $n = 2$ and 3 and $v_n^L/\sqrt{\langle \epsilon_n^2 \rangle}$ for $n = 4$ and 5 (denoted by "linear" in figure legend), with ϵ_n calculated in the MC Glauber model (left panel) and MC-KLN model (right panel). The higher-order flow harmonics show increasingly strong centrality dependence, which is consistent with the stronger viscous-damping effects, as expected from hydrodynamic model calculations [16,48,49]. For comparison, the ratios are also shown for the full v_4 and v_5 values without the linear and nonlinear decomposition, i.e., $v_4/\sqrt{\langle \epsilon_4^2 \rangle}$ (open diamonds) and
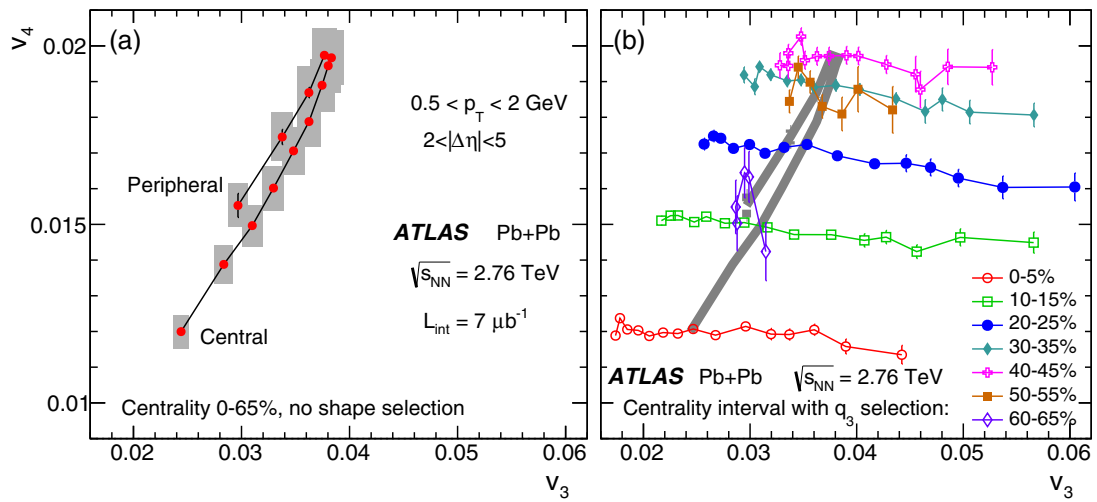
FIG. 12. (Color online) The correlation of v_3 (x axis) with v_4 (y axis), both measured in $0.5 < p_T < 2$ GeV. The left panel shows the v_3 and v_4 values in thirteen 5% centrality intervals over the centrality range 0%–65% without event-shape selection. The data points are connected to show the boomerang trend from central to peripheral collisions, as indicated. The right panel shows the v_3 and v_4 values for 14 q_3 selections (the two highest q_3 intervals in Fig. 1 are combined) in several centrality ranges (markers) with larger v_3 value corresponding to larger q_3 value; they are overlaid with the centrality dependence from the left panel. The error bars and shaded boxes represent the statistical and systematic uncertainties, respectively.

FIG. 13. (Color online) The correlation of v_2 (x axis) with v_5 (y axis) in $0.5 < p_T < 2$ GeV for 14 q_2 selections (the two highest q_2 intervals in Fig. 1 are combined) in nine 5% centrality intervals. The data are compared with the rescaled ϵ_2-ϵ_5 correlation from MC Glauber and MC-KLN models in the same centrality interval. The data are also parametrized with Eq. (19), taking into account both statistical and systematic uncertainties. The N_{part} dependence of the fit parameters is shown in the last two panels. The error bars and shaded bands represent the statistical and systematic uncertainties, respectively.

$v_5/\sqrt{\langle \epsilon_5^2 \rangle}$ (open crosses); they show much weaker centrality dependence owing to the dominance of nonlinear contributions to more peripheral collisions.

VI. CONCLUSION

Correlations between v_m coefficients for $m = 2$ or 3 in different p_T ranges, and the correlation between v_m and other
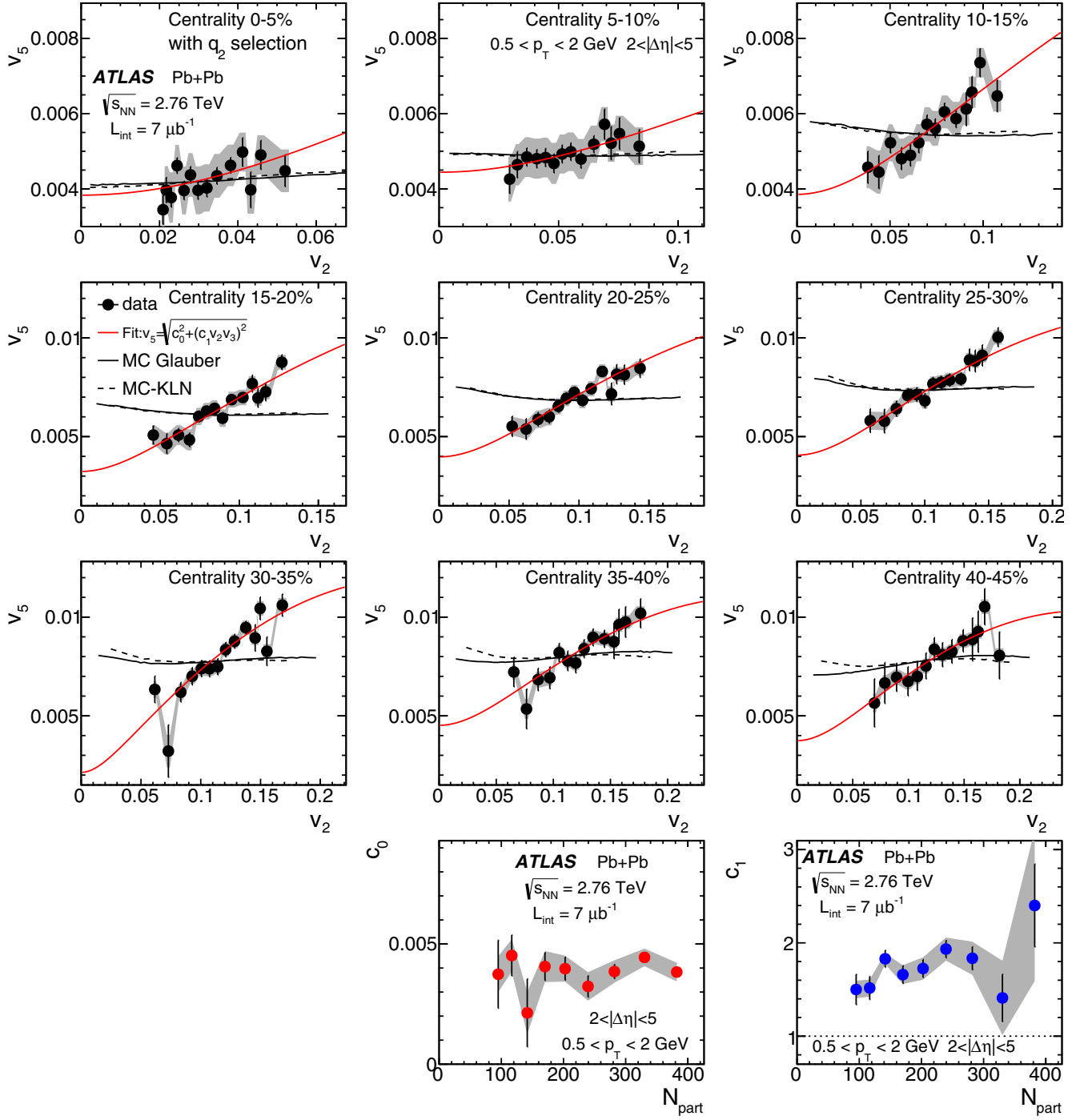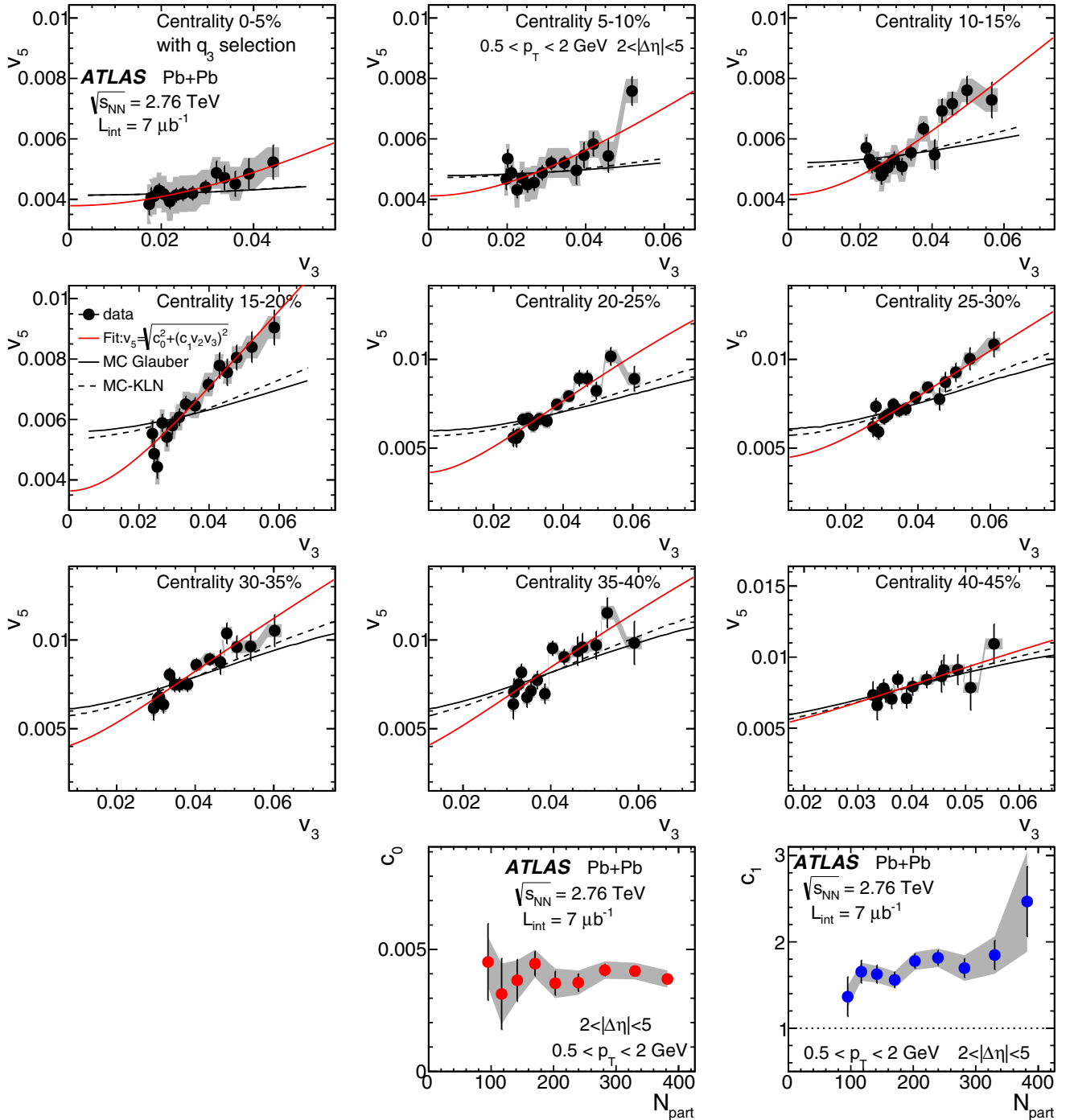
FIG. 14. (Color online) The correlation of v_3 (x axis) with v_5 (y axis) in $0.5 < p_T < 2$ GeV for 14 q_3 selections (the two highest q_3 intervals in Fig. 1 are combined) in nine 5% centrality intervals. The data are compared with the rescaled ϵ_3-ϵ_5 correlation from MC Glauber and MC-KLN models in the same centrality interval. The data are also parametrized with Eq. (19), taking into account both statistical and systematic uncertainties. The N_{part} dependence of the fit parameters is shown in the last two panels. The error bars and shaded bands represent the statistical and systematic uncertainties, respectively.

flow harmonics v_n for $n = 2$ to 5 in the same p_T range, are presented using 7 μb^{-1} of Pb + Pb collision data at $\sqrt{s_{NN}} = 2.76$ TeV collected in 2010 by the ATLAS experiment at the LHC. The v_m-v_n correlations are measured for events within a given narrow centrality interval using an event-shape selection method. Beside the centrality selection, this method makes a

further classification of events according to their raw elliptic flow signal q_2 or raw triangular flow signal q_3 in the forward rapidity range $3.3 < |\eta| < 4.8$. For each q_m bin, the v_m and v_n coefficients are calculated at midrapidity $|\eta| < 2.5$ using a two-particle correlation method, and hence the differential v_m-v_n correlation within each centrality interval can be obtained.
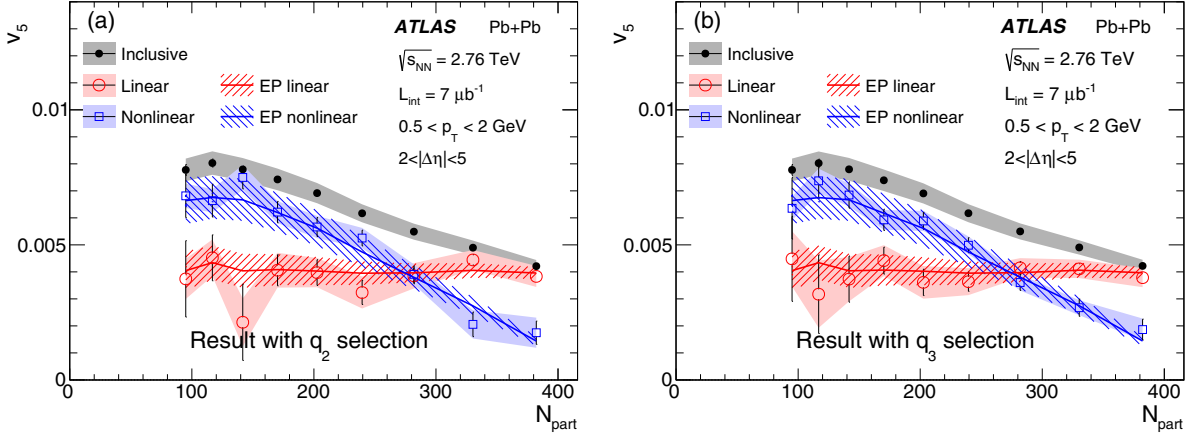
FIG. 15. (Color online) The centrality (N_{part}) dependence of the v_5 in $0.5 < p_T < 2\,\mathrm{GeV}$ and the associated linear and nonlinear components extracted from the fits in Figs. 13 and 14 and Eq. (20). They are compared with the linear and the nonlinear components estimated from the previous published EP correlation [14] via Eq. (21). The error bars represent the statistical uncertainties, while the shaded bands or hashed bands represent the systematic uncertainties.

The correlation of v_m between two different p_T ranges shows a complex centrality dependence, but within a narrow centrality interval the correlation varies linearly with the event shape as determined by q_2 or q_3. This linearity indicates that the viscous effects are controlled by the system size, not by its overall shape. An anticorrelation is observed between v_2 and v_3 within a given centrality interval and agrees qualitatively with similar anticorrelation between corresponding eccentricities ϵ_2 and ϵ_3, indicating that these correlations are associated with initial-geometry effects.
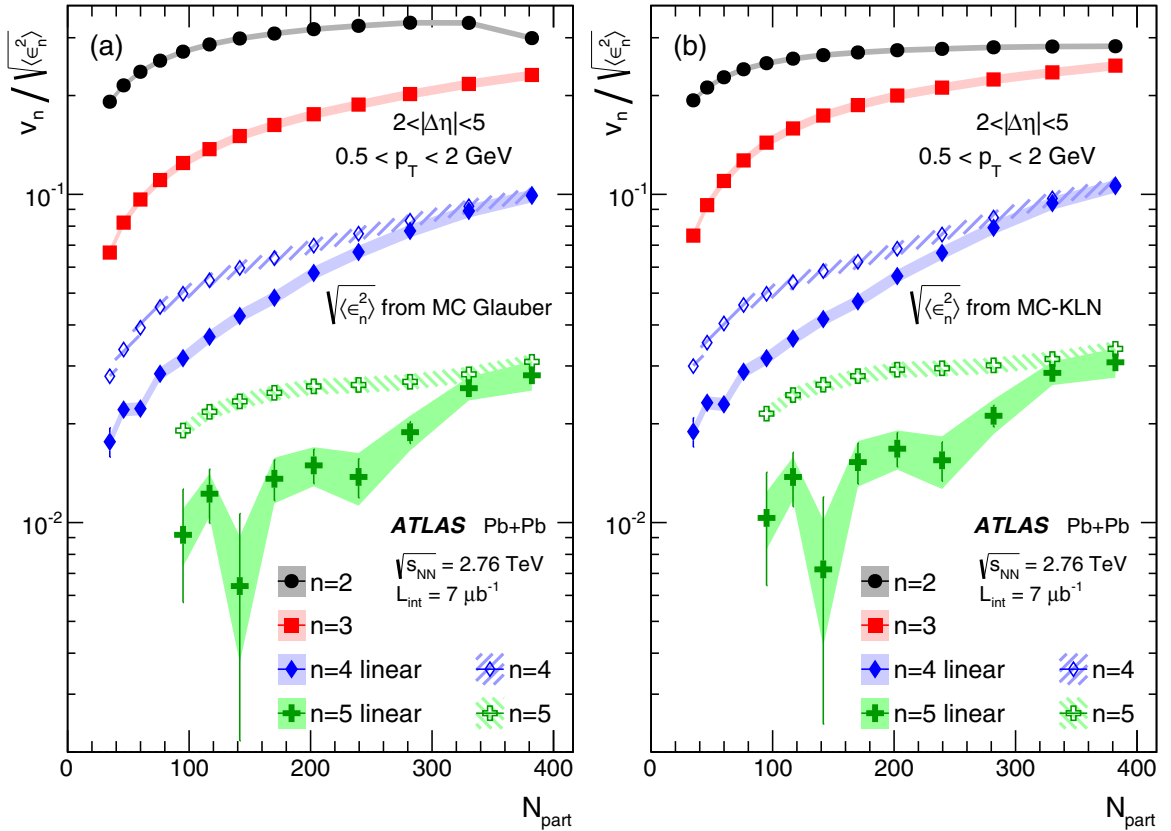
FIG. 16. (Color online) The eccentricity-scaled v_n or the estimated linear component v_n^{L} obtained from two-component fits, $v_2/\sqrt{\langle\epsilon_2^2\rangle}$ (circles), $v_3/\sqrt{\langle\epsilon_3^2\rangle}$ (boxes), $v_4^{\mathrm{L}}/\sqrt{\langle\epsilon_4^2\rangle}$ (solid diamonds), $v_5^{\mathrm{L}}/\sqrt{\langle\epsilon_5^2\rangle}$ (solid crosses), $v_4/\sqrt{\langle\epsilon_4^2\rangle}$ (open diamonds), and $v_5/\sqrt{\langle\epsilon_5^2\rangle}$ (open crosses). The eccentricities are calculated from the MC Glauber model (left) and the MC-KLN model (right). The error bars represent the statistical uncertainties, while the shaded bands or hashed bands represent the systematic uncertainties.

The v_4 is found to increase strongly with v_2, and v_5 is found to increase strongly with both v_2 and v_3 within a given centrality interval. The trends and the strengths of v_2-v_4, v_2-v_5, and v_3-v_5 correlations disagree with corresponding ϵ_m-ϵ_n correlations predicted by MC Glauber and MC-KLN initial-geometry models. Instead, these correlations are found to be consistent with a combination of a linear contribution to v_4 from ϵ_4 and to v_5 from ϵ_5, together with a nonlinear term that is a function of v_2^2 or of $v_2 v_3$, as predicted by hydrodynamic models [23,26]. The functional form of these nonlinear contributions is eclipsed in the overall centrality dependence, but has been directly exposed in the event-shape-selected measurements reported here. A simple two-component fit is used to separate these two contributions in v_4 and v_5. The extracted linear and nonlinear contributions are found to be consistent with those obtained from previously measured EP correlations.

To quantify the response of the medium to the initial geometry, the extracted linear components of v_4 and v_5, v_4^L and v_5^L, are scaled by the r.m.s. eccentricity of corresponding order. The scaled quantities, $v_4^L/\sqrt{\langle \epsilon_4^2 \rangle}$ and $v_5^L/\sqrt{\langle \epsilon_5^2 \rangle}$, show stronger centrality dependence than the similarly scaled quantities for elliptic flow and triangular flow, consistent with the stronger viscous-damping effects expected for higher-order harmonics.

ACKNOWLEDGMENTS

[1] M. Gyulassy, D. H. Rischke, and B. Zhang, Nucl. Phys. A **613**, 397 (1997).
[2] B. Alver *et al.* (PHOBOS Collaboration), Phys. Rev. Lett. **98**, 242302 (2007).
[3] J.-Y. Ollitrault, Phys. Rev. D **46**, 229 (1992).
[4] B. Alver and G. Roland, Phys. Rev. C **81**, 054905 (2010).
[5] C. Gale, S. Jeon, and B. Schenke, Int. J. Mod. Phys. A **28**, 1340011 (2013).
[6] U. Heinz and R. Snellings, Annu. Rev. Nucl. Part. Sci. **63**, 123 (2013).
[7] M. Luzum and H. Petersen, J. Phys. G **41**, 063102 (2014).
[8] A. Adare *et al.* (PHENIX Collaboration), Phys. Rev. Lett. **107**, 252301 (2011).
[9] L. Adamczyk *et al.* (STAR Collaboration), Phys. Rev. C **88**, 014904 (2013).
[10] K. Aamodt *et al.* (ALICE Collaboration), Phys. Rev. Lett. **107**, 032301 (2011).
[11] ATLAS Collaboration, Phys. Rev. C **86**, 014907 (2012).
[12] CMS Collaboration, Phys. Rev. C **89**, 044906 (2014).
[13] ATLAS Collaboration, J. High Energy Phys. 11 (2013) 183.
[14] ATLAS Collaboration, Phys. Rev. C **90**, 024905 (2014).
[15] M. Luzum and J.-Y. Ollitrault, Nucl. Phys. A **904-905**, 377c (2013).
[16] D. Teaney and L. Yan, Phys. Rev. C **83**, 064904 (2011).
[17] C. Gale, S. Jeon, B. Schenke, P. Tribedy, and R. Venugopalan, Phys. Rev. Lett. **110**, 012302 (2013).
[18] H. Niemi, G. S. Denicol, H. Holopainen, and P. Huovinen, Phys. Rev. C **87**, 054901 (2013).
[19] Z. Qiu and U. Heinz, Phys. Lett. B **717**, 261 (2012).
[20] D. Teaney and L. Yan, Phys. Rev. C **90**, 024902 (2014).
[21] S. A. Voloshin and Y. Zhang, Z. Phys. C **70**, 665 (1996).
[22] Z. Qiu and U. Heinz, Phys. Rev. C **84**, 024911 (2011).
[23] F. G. Gardim, F. Grassi, M. Luzum, and J.-Y. Ollitrault, Phys. Rev. C **85**, 024908 (2012).
[24] S. A. Voloshin, A. M. Poskanzer, and R. Snellings, arXiv:0809.2949 [nucl-ex].
[25] D. Teaney and L. Yan, Phys. Rev. C **86**, 044908 (2012).
[26] D. Teaney and L. Yan, Nucl. Phys. A **904**, 365c (2013).
[27] J. Schukraft, A. Timmins, and S. A. Voloshin, Phys. Lett. B **719**, 394 (2013).
[28] P. Huo, J. Jia, and S. Mohapatra, Phys. Rev. C **90**, 024910 (2014).
[29] R. A. Lacey *et al.*, arXiv:1311.1728 [nucl-ex].
[30] ATLAS Collaboration, J. Instrum. **3**, S08003 (2008).
[31] ATLAS Collaboration, Phys. Lett. B **707**, 330 (2012).
[32] ATLAS Collaboration, Phys. Lett. B **710**, 363 (2012).
[33] ATLAS Collaboration, Eur. Phys. J. C **73**, 2304 (2013).
[34] M. L. Miller, K. Reygers, S. J. Sanders, and P. Steinberg, Annu. Rev. Nucl. Part. Sci. **57**, 205 (2007).

[35] M. Gyulassy and X.-N. Wang, Comput. Phys. Commun. **83**, 307 (1994).

[36] M. Masera, G. Ortona, M. G. Poghosyan, and F. Prino, Phys. Rev. C **79**, 064909 (2009).

[37] S. Agostinelli *et al.* (GEANT4 Collaboration), Nucl. Instrum. Methods A **506**, 250 (2003).

[38] ATLAS Collaboration, Eur. Phys. J. C **70**, 823 (2010).

[39] A. M. Poskanzer and S. A. Voloshin, Phys. Rev. C **58**, 1671 (1998).

[40] S. Afanasiev *et al.* (PHENIX Collaboration), Phys. Rev. C **80**, 024909 (2009).

[41] J. Barrette *et al.* (E877 Collaboration), Phys. Rev. C **56**, 3254 (1997).

[42] CMS Collaboration, J. High Energy Phys. 02 (2014) 088.

[43] K. Adcox *et al.* (PHENIX Collaboration), Phys. Rev. Lett. **89**, 212301 (2002).

[44] K. Aamodt *et al.* (ALICE Collaboration), Phys. Lett. B **708**, 249 (2012).

[45] M. Luzum and P. Romatschke, Phys. Rev. C **78**, 034915 (2008).

[46] Z.-W. Lin, C. M. Ko, B.-A. Li, B. Zhang, and S. Pal, Phys. Rev. C **72**, 064901 (2005).

[47] A. Adil, H.-J. Drescher, A. Dumitru, A. Hayashigaki, and Y. Nara, Phys. Rev. C **74**, 044905 (2006).

[48] B. H. Alver, C. Gombeaud, M. Luzum, and J.-Y. Ollitrault, Phys. Rev. C **82**, 034913 (2010).

[49] B. Schenke, S. Jeon, and C. Gale, Phys. Rev. C **85**, 024901 (2012).

G. Aad,[85] B. Abbott,[113] J. Abdallah,[151] O. Abdinov,[11] R. Aben,[107] M. Abolins,[90] O. S. AbouZeid,[158] H. Abramowicz,[153] H. Abreu,[152] R. Abreu,[30] Y. Abulaiti,[146a,146b] B. S. Acharya,[164a,164b,a] L. Adamczyk,[38a] D. L. Adams,[25] J. Adelman,[108] S. Adomeit,[100] T. Adye,[131] A. A. Affolder,[74] T. Agatonovic-Jovin,[13] J. A. Aguilar-Saavedra,[126a,126f] S. P. Ahlen,[22] F. Ahmadov,[65,b] G. Aielli,[133a,133b] H. Akerstedt,[146a,146b] T. P. A. Åkesson,[81] G. Akimoto,[155] A. V. Akimov,[96] G. L. Alberghi,[20a,20b] J. Albert,[169] S. Albrand,[55] M. J. Alconada Verzini,[71] M. Aleksa,[30] I. N. Aleksandrov,[65] C. Alexa,[26a] G. Alexander,[153] T. Alexopoulos,[10] M. Alhroob,[113] G. Alimonti,[91a] L. Alio,[85] J. Alison,[31] S. P. Alkire,[35] B. M. M. Allbrooke,[18] P. P. Allport,[74] A. Aloisio,[104a,104b] A. Alonso,[36] F. Alonso,[71] C. Alpigiani,[76] A. Altheimer,[35] B. Alvarez Gonzalez,[30] D. Álvarez Piqueras,[167] M. G. Alviggi,[104a,104b] B. T. Amadio,[15] K. Amako,[66] Y. Amaral Coutinho,[24a] C. Amelung,[23] D. Amidei,[89] S. P. Amor Dos Santos,[126a,126c] A. Amorim,[126a,126b] S. Amoroso,[48] N. Amram,[153] G. Amundsen,[23] C. Anastopoulos,[139] L. S. Ancu,[49] N. Andari,[30] T. Andeen,[35] C. F. Anders,[58b] G. Anders,[30] J. K. Anders,[74] K. J. Anderson,[31] A. Andreazza,[91a,91b] V. Andrei,[58a] S. Angelidakis,[9] I. Angelozzi,[107] P. Anger,[44] A. Angerami,[35] F. Anghinolfi,[30] A. V. Anisenkov,[109,c] N. Anjos,[12] A. Annovi,[124a,124b] M. Antonelli,[47] A. Antonov,[98] J. Antos,[144b] F. Anulli,[132a] M. Aoki,[66] L. Aperio Bella,[18] G. Arabidze,[90] Y. Arai,[66] J. P. Araque,[126a] A. T. H. Arce,[45] F. A. Arduh,[71] J-F. Arguin,[95] S. Argyropoulos,[42] M. Arik,[19a] A. J. Armbruster,[30] O. Arnaez,[30] V. Arnal,[82] H. Arnold,[48] M. Arratia,[28] O. Arslan,[21] A. Artamonov,[97] G. Artoni,[23] S. Asai,[155] N. Asbah,[42] A. Ashkenazi,[153] B. Åsman,[146a,146b] L. Asquith,[149] K. Assamagan,[25] R. Astalos,[144a] M. Atkinson,[165] N. B. Atlay,[141] B. Auerbach,[6] K. Augsten,[128] M. Aurousseau,[145b] G. Avolio,[30] B. Axen,[15] M. K. Ayoub,[117] G. Azuelos,[95,d] M. A. Baak,[30] A. E. Baas,[58a] C. Bacci,[134a,134b] H. Bachacou,[136] K. Bachas,[154] M. Backes,[30] M. Backhaus,[30] E. Badescu,[26a] P. Bagiacchi,[132a,132b] P. Bagnaia,[132a,132b] Y. Bai,[33a] T. Bain,[35] J. T. Baines,[131] O. K. Baker,[176] P. Balek,[129] T. Balestri,[148] F. Balli,[84] E. Banas,[39] Sw. Banerjee,[173] A. A. E. Bannoura,[175] H. S. Bansil,[18] L. Barak,[30] S. P. Baranov,[96] E. L. Barberio,[88] D. Barberis,[50a,50b] M. Barbero,[85] T. Barillari,[101] M. Barisonzi,[164a,164b] T. Barklow,[143] N. Barlow,[28] S. L. Barnes,[84] B. M. Barnett,[131] R. M. Barnett,[15] Z. Barnovska,[5] A. Baroncelli,[134a] G. Barone,[49] A. J. Barr,[120] F. Barreiro,[82] J. Barreiro Guimarães da Costa,[57] R. Bartoldus,[143] A. E. Barton,[72] P. Bartos,[144a] A. Bassalat,[117] A. Basye,[165] R. L. Bates,[53] S. J. Batista,[158] J. R. Batley,[28] M. Battaglia,[137] M. Bauce,[132a,132b] F. Bauer,[136] H. S. Bawa,[143,e] J. B. Beacham,[111] M. D. Beattie,[72] T. Beau,[80] P. H. Beauchemin,[161] R. Beccherle,[124a,124b] P. Bechtle,[21] H. P. Beck,[17,f] K. Becker,[120] M. Becker,[83] S. Becker,[100] M. Beckingham,[170] C. Becot,[117] A. J. Beddall,[19c] A. Beddall,[19c] V. A. Bednyakov,[65] C. P. Bee,[148] L. J. Beemster,[107] T. A. Beermann,[175] M. Begel,[25] J. K. Behr,[120] C. Belanger-Champagne,[87] W. H. Bell,[49] G. Bella,[153] L. Bellagamba,[20a] A. Bellerive,[29] M. Bellomo,[86] K. Belotskiy,[98] O. Beltramello,[30] O. Benary,[153] D. Benchekroun,[135a] M. Bender,[100] K. Bendtz,[146a,146b] N. Benekos,[10] Y. Benhammou,[153] E. Benhar Noccioli,[49] J. A. Benitez Garcia,[159b] D. P. Benjamin,[45] J. R. Bensinger,[23] S. Bentvelsen,[107] L. Beresford,[120] M. Beretta,[47] D. Berge,[107] E. Bergeaas Kuutmann,[166] N. Berger,[5] F. Berghaus,[169] J. Beringer,[15] C. Bernard,[22] N. R. Bernard,[86] C. Bernius,[110] F. U. Bernlochner,[21] T. Berry,[77] P. Berta,[129] C. Bertella,[83] G. Bertoli,[146a,146b] F. Bertolucci,[124a,124b] C. Bertsche,[113] D. Bertsche,[113] M. I. Besana,[91a] G. J. Besjes,[106] O. Bessidskaia Bylund,[146a,146b] M. Bessner,[42] N. Besson,[136] C. Betancourt,[48] S. Bethke,[101] A. J. Bevan,[76] W. Bhimji,[46] R. M. Bianchi,[125] L. Bianchini,[23] M. Bianco,[30] O. Biebel,[100] S. P. Bieniek,[78] M. Biglietti,[134a] J. Bilbao De Mendizabal,[49] H. Bilokon,[47] M. Bindi,[54] S. Binet,[117] A. Bingul,[19c] C. Bini,[132a,132b] C. W. Black,[150] J. E. Black,[143] K. M. Black,[22] D. Blackburn,[138] R. E. Blair,[6] J.-B. Blanchard,[136] J. E. Blanco,[77] T. Blazek,[144a] I. Bloch,[42] C. Blocker,[23] W. Blum,[83,*] U. Blumenschein,[54] G. J. Bobbink,[107] V. S. Bobrovnikov,[109,c] S. S. Bocchetta,[81] A. Bocci,[45] C. Bock,[100] M. Boehler,[48] J. A. Bogaerts,[30] A. G. Bogdanchikov,[109] C. Bohm,[146a] V. Boisvert,[77] T. Bold,[38a] V. Boldea,[26a] A. S. Boldyrev,[99] M. Bomben,[80] M. Bona,[76] M. Boonekamp,[136] A. Borisov,[130] G. Borissov,[72] S. Borroni,[42] J. Bortfeldt,[100] V. Bortolotto,[60a,60b,60c] K. Bos,[107] D. Boscherini,[20a] M. Bosman,[12] J. Boudreau,[125] J. Bouffard,[2] E. V. Bouhova-Thacker,[72] D. Boumediene,[34] C. Bourdarios,[117] N. Bousson,[114] A. Boveia,[30] J. Boyd,[30] I. R. Boyko,[65] I. Bozic,[13] J. Bracinik,[18] A. Brandt,[8] G. Brandt,[54]

O. Brandt,[58a] U. Bratzler,[156] B. Brau,[86] J. E. Brau,[116] H. M. Braun,[175,*] S. F. Brazzale,[164a,164c] K. Brendlinger,[122] A. J. Brennan,[88] L. Brenner,[107] R. Brenner,[166] S. Bressler,[172] K. Bristow,[145c] T. M. Bristow,[46] D. Britton,[53] D. Britzger,[42] F. M. Brochu,[28] I. Brock,[21] R. Brock,[90] J. Bronner,[101] G. Brooijmans,[35] T. Brooks,[77] W. K. Brooks,[32b] J. Brosamer,[15] E. Brost,[116] J. Brown,[55] P. A. Bruckman de Renstrom,[39] D. Bruncko,[144b] R. Bruneliere,[48] A. Bruni,[20a] G. Bruni,[20a] M. Bruschi,[20a] L. Bryngemark,[81] T. Buanes,[14] Q. Buat,[142] P. Buchholz,[141] A. G. Buckley,[53] S. I. Buda,[26a] I. A. Budagov,[65] F. Buehrer,[48] L. Bugge,[119] M. K. Bugge,[119] O. Bulekov,[98] D. Bullock,[8] H. Burckhart,[30] S. Burdin,[74] B. Burghgrave,[108] S. Burke,[131] I. Burmeister,[43] E. Busato,[34] D. Büscher,[48] V. Büscher,[83] P. Bussey,[53] C. P. Buszello,[166] J. M. Butler,[22] A. I. Butt,[3] C. M. Buttar,[53] J. M. Butterworth,[78] P. Butti,[107] W. Buttinger,[25] A. Buzatu,[53] R. Buzykaev,[109,c] S. Cabrera Urbán,[167] D. Caforio,[128] V. M. Cairo,[37a,37b] O. Cakir,[4a] P. Calafiura,[15] A. Calandri,[136] G. Calderini,[80] P. Calfayan,[100] L. P. Caloba,[24a] D. Calvet,[34] S. Calvet,[34] R. Camacho Toro,[31] S. Camarda,[42] P. Camarri,[133a,133b] D. Cameron,[119] L. M. Caminada,[15] R. Caminal Armadans,[12] S. Campana,[30] M. Campanelli,[78] A. Campoverde,[148] V. Canale,[104a,104b] A. Canepa,[159a] M. Cano Bret,[76] J. Cantero,[82] R. Cantrill,[126a] T. Cao,[40] M. D. M. Capeans Garrido,[30] I. Caprini,[26a] M. Caprini,[26a] M. Capua,[37a,37b] R. Caputo,[83] R. Cardarelli,[133a] T. Carli,[30] G. Carlino,[104a] L. Carminati,[91a,91b] S. Caron,[106] E. Carquin,[32a] G. D. Carrillo-Montoya,[8] J. R. Carter,[28] J. Carvalho,[126a,126c] D. Casadei,[78] M. P. Casado,[12] M. Casolino,[12] E. Castaneda-Miranda,[145b] A. Castelli,[107] V. Castillo Gimenez,[167] N. F. Castro,[126a,g] P. Catastini,[57] A. Catinaccio,[30] J. R. Catmore,[119] A. Cattai,[30] J. Caudron,[83] V. Cavaliere,[165] D. Cavalli,[91a] M. Cavalli-Sforza,[12] V. Cavasinni,[124a,124b] F. Ceradini,[134a,134b] B. C. Cerio,[45] K. Cerny,[129] A. S. Cerqueira,[24b] A. Cerri,[149] L. Cerrito,[76] F. Cerutti,[15] M. Cerv,[30] A. Cervelli,[17] S. A. Cetin,[19b] A. Chafaq,[135a] D. Chakraborty,[108] I. Chalupkova,[129] P. Chang,[165] B. Chapleau,[87] J. D. Chapman,[28] D. G. Charlton,[18] C. C. Chau,[158] C. A. Chavez Barajas,[149] S. Cheatham,[152] A. Chegwidden,[90] S. Chekanov,[6] S. V. Chekulaev,[159a] G. A. Chelkov,[65,h] M. A. Chelstowska,[89] C. Chen,[64] H. Chen,[25] K. Chen,[148] L. Chen,[33d,i] S. Chen,[33c] X. Chen,[33f] Y. Chen,[67] H. C. Cheng,[89] Y. Cheng,[31] A. Cheplakov,[65] E. Cheremushkina,[130] R. Cherkaoui El Moursli,[135e] V. Chernyatin,[25,*] E. Cheu,[7] L. Chevalier,[136] V. Chiarella,[47] J. T. Childers,[6] G. Chiodini,[73a] A. S. Chisholm,[18] R. T. Chislett,[78] A. Chitan,[26a] M. V. Chizhov,[65] K. Choi,[61] S. Chouridou,[9] B. K. B. Chow,[100] V. Christodoulou,[78] D. Chromek-Burckhart,[30] M. L. Chu,[151] J. Chudoba,[127] A. J. Chuinard,[87] J. J. Chwastowski,[39] L. Chytka,[115] G. Ciapetti,[132a,132b] A. K. Ciftci,[4a] D. Cinca,[53] V. Cindro,[75] I. A. Cioara,[21] A. Ciocio,[15] Z. H. Citron,[172] M. Ciubancan,[26a] A. Clark,[49] B. L. Clark,[57] P. J. Clark,[46] R. N. Clarke,[15] W. Cleland,[125] C. Clement,[146a,146b] Y. Coadou,[85] M. Cobal,[164a,164c] A. Coccaro,[138] J. Cochran,[64] L. Coffey,[23] J. G. Cogan,[143] B. Cole,[35] S. Cole,[108] A. P. Colijn,[107] J. Collot,[55] T. Colombo,[58c] G. Compostella,[101] P. Conde Muiño,[126a,126b] E. Coniavitis,[48] S. H. Connell,[145b] I. A. Connelly,[77] S. M. Consonni,[91a,91b] V. Consorti,[48] S. Constantinescu,[26a] C. Conta,[121a,121b] G. Conti,[30] F. Conventi,[104a,j] M. Cooke,[15] B. D. Cooper,[78] A. M. Cooper-Sarkar,[120] T. Cornelissen,[175] M. Corradi,[20a] F. Corriveau,[87,k] A. Corso-Radu,[163] A. Cortes-Gonzalez,[12] G. Cortiana,[101] G. Costa,[91a] M. J. Costa,[167] D. Costanzo,[139] D. Côté,[8] G. Cottin,[28] G. Cowan,[77] B. E. Cox,[84] K. Cranmer,[110] G. Cree,[29] S. Crépé-Renaudin,[55] F. Crescioli,[80] W. A. Cribbs,[146a,146b] M. Crispin Ortuzar,[120] M. Cristinziani,[21] V. Croft,[106] G. Crosetti,[37a,37b] T. Cuhadar Donszelmann,[139] J. Cummings,[176] M. Curatolo,[47] C. Cuthbert,[150] H. Czirr,[141] P. Czodrowski,[3] S. D'Auria,[53] M. D'Onofrio,[74] M. J. Da Cunha Sargedas De Sousa,[126a,126b] C. Da Via,[84] W. Dabrowski,[38a] A. Dafinca,[120] T. Dai,[89] O. Dale,[14] F. Dallaire,[95] C. Dallapiccola,[86] M. Dam,[36] J. R. Dandoy,[31] N. P. Dang,[48] A. C. Daniells,[18] M. Danninger,[168] M. Dano Hoffmann,[136] V. Dao,[48] G. Darbo,[50a] S. Darmora,[8] J. Dassoulas,[3] A. Dattagupta,[61] W. Davey,[21] C. David,[169] T. Davidek,[129] E. Davies,[120,l] M. Davies,[153] P. Davison,[78] Y. Davygora,[58a] E. Dawe,[88] I. Dawson,[139] R. K. Daya-Ishmukhametova,[86] K. De,[8] R. de Asmundis,[104a] S. De Castro,[20a,20b] S. De Cecco,[80] N. De Groot,[106] P. de Jong,[107] H. De la Torre,[82] F. De Lorenzi,[64] L. De Nooij,[107] D. De Pedis,[132a] A. De Salvo,[132a] U. De Sanctis,[149] A. De Santo,[149] J. B. De Vivie De Regie,[117] W. J. Dearnaley,[72] R. Debbe,[25] C. Debenedetti,[137] D. V. Dedovich,[65] I. Deigaard,[107] J. Del Peso,[82] T. Del Prete,[124a,124b] D. Delgove,[117] F. Deliot,[136] C. M. Delitzsch,[49] M. Deliyergiyev,[75] A. Dell'Acqua,[30] L. Dell'Asta,[22] M. Dell'Orso,[124a,124b] M. Della Pietra,[104a,j] D. della Volpe,[49] M. Delmastro,[5] P. A. Delsart,[55] C. Deluca,[107] D. A. DeMarco,[158] S. Demers,[176] M. Demichev,[65] A. Demilly,[80] S. P. Denisov,[130] D. Derendarz,[39] J. E. Derkaoui,[135d] F. Derue,[80] P. Dervan,[74] K. Desch,[21] C. Deterre,[42] P. O. Deviveiros,[30] A. Dewhurst,[131] S. Dhaliwal,[107] A. Di Ciaccio,[133a,133b] L. Di Ciaccio,[5] A. Di Domenico,[132a,132b] C. Di Donato,[104a,104b] A. Di Girolamo,[30] B. Di Girolamo,[30] A. Di Mattia,[152] B. Di Micco,[134a,134b] R. Di Nardo,[47] A. Di Simone,[48] R. Di Sipio,[158] D. Di Valentino,[29] C. Diaconu,[85] M. Diamond,[158] F. A. Dias,[46] M. A. Diaz,[32a] E. B. Diehl,[89] J. Dietrich,[16] S. Diglio,[85] A. Dimitrievska,[13] J. Dingfelder,[21] P. Dita,[26a] S. Dita,[26a] F. Dittus,[30] F. Djama,[85] T. Djobava,[51b] J. I. Djuvsland,[58a] M. A. B. do Vale,[24c] D. Dobos,[30] M. Dobre,[26a] C. Doglioni,[49] T. Dohmae,[155] J. Dolejsi,[129] Z. Dolezal,[129] B. A. Dolgoshein,[98,*] M. Donadelli,[24d] S. Donati,[124a,124b] P. Dondero,[121a,121b] J. Donini,[34] J. Dopke,[131] A. Doria,[104a] M. T. Dova,[71] A. T. Doyle,[53] E. Drechsler,[54] M. Dris,[10] E. Dubreuil,[34] E. Duchovni,[172] G. Duckeck,[100] O. A. Ducu,[26a,85] D. Duda,[175] A. Dudarev,[30] L. Duflot,[117] L. Duguid,[77] M. Dührssen,[30] M. Dunford,[58a] H. Duran Yildiz,[4a] M. Düren,[52] A. Durglishvili,[51b] D. Duschinger,[44] M. Dyndal,[38a] C. Eckardt,[42] K. M. Ecker,[101] R. C. Edgar,[89] W. Edson,[2] N. C. Edwards,[46] W. Ehrenfeld,[21] T. Eifert,[30] G. Eigen,[14] K. Einsweiler,[15] T. Ekelof,[166] M. El Kacimi,[135c] M. Ellert,[166] S. Elles,[5] F. Ellinghaus,[83] A. A. Elliot,[169] N. Ellis,[30] J. Elmsheuser,[100] M. Elsing,[30] D. Emeliyanov,[131] Y. Enari,[155] O. C. Endner,[83] M. Endo,[118] R. Engelmann,[148] J. Erdmann,[43] A. Ereditato,[17] G. Ernis,[175] J. Ernst,[2] M. Ernst,[25] S. Errede,[165] E. Ertel,[83] M. Escalier,[117] H. Esch,[43] C. Escobar,[125] B. Esposito,[47] A. I. Etienvre,[136] E. Etzion,[153] H. Evans,[61] A. Ezhilov,[123] L. Fabbri,[20a,20b] G. Facini,[31] R. M. Fakhrutdinov,[130] S. Falciano,[132a] R. J. Falla,[78] J. Faltova,[129] Y. Fang,[33a] M. Fanti,[91a,91b] A. Farbin,[8] A. Farilla,[134a] T. Farooque,[12] S. Farrell,[15] S. M. Farrington,[170] P. Farthouat,[30] F. Fassi,[135e] P. Fassnacht,[30] D. Fassouliotis,[9] M. Faucci Giannelli,[77] A. Favareto,[50a,50b] L. Fayard,[117] P. Federic,[144a] O. L. Fedin,[123,m] W. Fedorko,[168]

S. Feigl,[30] L. Feligioni,[85] C. Feng,[33d] E. J. Feng,[6] H. Feng,[89] A. B. Fenyuk,[130] P. Fernandez Martinez,[167] S. Fernandez Perez,[30] S. Ferrag,[53] J. Ferrando,[53] A. Ferrari,[166] P. Ferrari,[107] R. Ferrari,[121a] D. E. Ferreira de Lima,[53] A. Ferrer,[167] D. Ferrere,[49] C. Ferretti,[89] A. Ferretto Parodi,[50a,50b] M. Fiascaris,[31] F. Fiedler,[83] A. Filipčič,[75] M. Filipuzzi,[42] F. Filthaut,[106] M. Fincke-Keeler,[169] K. D. Finelli,[150] M. C. N. Fiolhais,[126a,126c] L. Fiorini,[167] A. Firan,[40] A. Fischer,[2] C. Fischer,[12] J. Fischer,[175] W. C. Fisher,[90] E. A. Fitzgerald,[23] M. Flechl,[48] I. Fleck,[141] P. Fleischmann,[89] S. Fleischmann,[175] G. T. Fletcher,[139] G. Fletcher,[76] T. Flick,[175] A. Floderus,[81] L. R. Flores Castillo,[60a] M. J. Flowerdew,[101] A. Formica,[136] A. Forti,[84] D. Fournier,[117] H. Fox,[72] S. Fracchia,[12] P. Francavilla,[80] M. Franchini,[20a,20b] D. Francis,[30] L. Franconi,[119] M. Franklin,[57] M. Fraternali,[121a,121b] D. Freeborn,[78] S. T. French,[28] F. Friedrich,[44] D. Froidevaux,[30] J. A. Frost,[120] C. Fukunaga,[156] E. Fullana Torregrosa,[83] B. G. Fulsom,[143] J. Fuster,[167] C. Gabaldon,[55] O. Gabizon,[175] A. Gabrielli,[20a,20b] A. Gabrielli,[132a,132b] S. Gadatsch,[107] S. Gadomski,[49] G. Gagliardi,[50a,50b] P. Gagnon,[61] C. Galea,[106] B. Galhardo,[126a,126c] E. J. Gallas,[120] B. J. Gallop,[131] P. Gallus,[128] G. Galster,[36] K. K. Gan,[111] J. Gao,[33b,85] Y. Gao,[46] Y. S. Gao,[143,e] F. M. Garay Walls,[46] F. Garberson,[176] C. García,[167] J. E. García Navarro,[167] M. Garcia-Sciveres,[15] R. W. Gardner,[31] N. Garelli,[143] V. Garonne,[119] C. Gatti,[47] A. Gaudiello,[50a,50b] G. Gaudio,[121a] B. Gaur,[141] L. Gauthier,[95] P. Gauzzi,[132a,132b] I. L. Gavrilenko,[96] C. Gay,[168] G. Gaycken,[21] E. N. Gazis,[10] P. Ge,[33d] Z. Gecse,[168] C. N. P. Gee,[131] D. A. A. Geerts,[107] Ch. Geich-Gimbel,[21] M. P. Geisler,[58a] C. Gemme,[50a] M. H. Genest,[55] S. Gentile,[132a,132b] M. George,[54] S. George,[77] D. Gerbaudo,[163] A. Gershon,[153] H. Ghazlane,[135b] B. Giacobbe,[20a] S. Giagu,[132a,132b] V. Giangiobbe,[12] P. Giannetti,[124a,124b] B. Gibbard,[25] S. M. Gibson,[77] M. Gilchriese,[15] T. P. S. Gillam,[28] D. Gillberg,[30] G. Gilles,[34] D. M. Gingrich,[3,d] N. Giokaris,[9] M. P. Giordani,[164a,164c] F. M. Giorgi,[20a] F. M. Giorgi,[16] P. F. Giraud,[136] P. Giromini,[47] D. Giugni,[91a] C. Giuliani,[48] M. Giulini,[58b] B. K. Gjelsten,[119] S. Gkaitatzis,[154] I. Gkialas,[154] E. L. Gkougkousis,[117] L. K. Gladilin,[99] C. Glasman,[82] J. Glatzer,[30] P. C. F. Glaysher,[46] A. Glazov,[42] M. Goblirsch-Kolb,[101] J. R. Goddard,[76] J. Godlewski,[39] S. Goldfarb,[89] T. Golling,[49] D. Golubkov,[130] A. Gomes,[126a,126b,126d] R. Gonçalo,[126a] J. Goncalves Pinto Firmino Da Costa,[136] L. Gonella,[21] S. González de la Hoz,[167] G. Gonzalez Parra,[12] S. Gonzalez-Sevilla,[49] L. Goossens,[30] P. A. Gorbounov,[97] H. A. Gordon,[25] I. Gorelov,[105] B. Gorini,[30] E. Gorini,[73a,73b] A. Gorišek,[75] E. Gornicki,[39] A. T. Goshaw,[45] C. Gössling,[43] M. I. Gostkin,[65] D. Goujdami,[135c] A. G. Goussiou,[138] N. Govender,[145b] H. M. X. Grabas,[137] L. Graber,[54] I. Grabowska-Bold,[38a] P. Grafström,[20a,20b] K-J. Grahn,[42] J. Gramling,[49] E. Gramstad,[119] S. Grancagnolo,[16] V. Grassi,[148] V. Gratchev,[123] H. M. Gray,[30] E. Graziani,[134a] Z. D. Greenwood,[79,n] K. Gregersen,[78] I. M. Gregor,[42] P. Grenier,[143] J. Griffiths,[8] A. A. Grillo,[137] K. Grimm,[72] S. Grinstein,[12,o] Ph. Gris,[34] J.-F. Grivaz,[117] J. P. Grohs,[44] A. Grohsjean,[42] E. Gross,[172] J. Grosse-Knetter,[54] G. C. Grossi,[79] Z. J. Grout,[149] L. Guan,[33b] J. Guenther,[128] F. Guescini,[49] D. Guest,[176] O. Gueta,[153] E. Guido,[50a,50b] T. Guillemin,[117] S. Guindon,[2] U. Gul,[53] C. Gumpert,[44] J. Guo,[33e] S. Gupta,[120] P. Gutierrez,[113] N. G. Gutierrez Ortiz,[53] C. Gutschow,[44] C. Guyot,[136] C. Gwenlan,[120] C. B. Gwilliam,[74] A. Haas,[110] C. Haber,[15] H. K. Hadavand,[8] N. Haddad,[135e] P. Haefner,[21] S. Hageböck,[21] Z. Hajduk,[39] H. Hakobyan,[177] M. Haleem,[42] J. Haley,[114] D. Hall,[120] G. Halladjian,[90] G. D. Hallewell,[85] K. Hamacher,[175] P. Hamal,[115] K. Hamano,[169] M. Hamer,[54] A. Hamilton,[145a] G. N. Hamity,[145c] P. G. Hamnett,[42] L. Han,[33b] K. Hanagaki,[118] K. Hanawa,[155] M. Hance,[15] P. Hanke,[58a] R. Hanna,[136] J. B. Hansen,[36] J. D. Hansen,[36] M. C. Hansen,[21] P. H. Hansen,[36] K. Hara,[160] A. S. Hard,[173] T. Harenberg,[175] F. Hariri,[117] S. Harkusha,[92] R. D. Harrington,[46] P. F. Harrison,[170] F. Hartjes,[107] M. Hasegawa,[67] S. Hasegawa,[103] Y. Hasegawa,[140] A. Hasib,[113] S. Hassani,[136] S. Haug,[17] R. Hauser,[90] L. Hauswald,[44] M. Havranek,[127] C. M. Hawkes,[18] R. J. Hawkings,[30] A. D. Hawkins,[81] T. Hayashi,[160] D. Hayden,[90] C. P. Hays,[120] J. M. Hays,[76] H. S. Hayward,[74] S. J. Haywood,[131] S. J. Head,[18] T. Heck,[83] V. Hedberg,[81] L. Heelan,[8] S. Heim,[122] T. Heim,[175] B. Heinemann,[15] L. Heinrich,[110] J. Hejbal,[127] L. Helary,[22] S. Hellman,[146a,146b] D. Hellmich,[21] C. Helsens,[30] J. Henderson,[120] R. C. W. Henderson,[72] Y. Heng,[173] C. Hengler,[42] A. Henrichs,[176] A. M. Henriques Correia,[30] S. Henrot-Versille,[117] G. H. Herbert,[16] Y. Hernández Jiménez,[167] R. Herrberg-Schubert,[16] G. Herten,[48] R. Hertenberger,[100] L. Hervas,[30] G. G. Hesketh,[78] N. P. Hessey,[107] J. W. Hetherly,[40] R. Hickling,[76] E. Higón-Rodriguez,[167] E. Hill,[169] J. C. Hill,[28] K. H. Hiller,[42] S. J. Hillier,[18] I. Hinchliffe,[15] E. Hines,[122] R. R. Hinman,[15] M. Hirose,[157] D. Hirschbuehl,[175] J. Hobbs,[148] N. Hod,[107] M. C. Hodgkinson,[139] P. Hodgson,[139] A. Hoecker,[30] M. R. Hoeferkamp,[105] F. Hoenig,[100] M. Hohlfeld,[83] D. Hohn,[21] T. R. Holmes,[15] T. M. Hong,[122] L. Hooft van Huysduynen,[110] W. H. Hopkins,[116] Y. Horii,[103] A. J. Horton,[142] J-Y. Hostachy,[55] S. Hou,[151] A. Hoummada,[135a] J. Howard,[120] J. Howarth,[42] M. Hrabovsky,[115] I. Hristova,[16] J. Hrivnac,[117] T. Hryn'ova,[5] A. Hrynevich,[93] C. Hsu,[145c] P. J. Hsu,[151,p] S.-C. Hsu,[138] D. Hu,[35] Q. Hu,[33b] X. Hu,[89] Y. Huang,[42] Z. Hubacek,[30] F. Hubaut,[85] F. Huegging,[21] T. B. Huffman,[120] E. W. Hughes,[35] G. Hughes,[72] M. Huhtinen,[30] T. A. Hülsing,[83] N. Huseynov,[65,b] J. Huston,[90] J. Huth,[57] G. Iacobucci,[49] G. Iakovidis,[25] I. Ibragimov,[141] L. Iconomidou-Fayard,[117] E. Ideal,[176] Z. Idrissi,[135e] P. Iengo,[30] O. Igonkina,[107] T. Iizawa,[171] Y. Ikegami,[66] K. Ikematsu,[141] M. Ikeno,[66] Y. Ilchenko,[31,q] D. Iliadis,[154] N. Ilic,[143] Y. Inamaru,[67] T. Ince,[101] P. Ioannou,[9] M. Iodice,[134a] K. Iordanidou,[35] V. Ippolito,[57] A. Irles Quiles,[167] C. Isaksson,[166] M. Ishino,[68] M. Ishitsuka,[157] R. Ishmukhametov,[111] C. Issever,[120] S. Istin,[19a] J. M. Iturbe Ponce,[84] R. Iuppa,[133a,133b] J. Ivarsson,[81] W. Iwanski,[39] H. Iwasaki,[66] J. M. Izen,[41] V. Izzo,[104a] S. Jabbar,[3] B. Jackson,[122] M. Jackson,[74] P. Jackson,[1] M. R. Jaekel,[30] V. Jain,[2] K. Jakobs,[48] S. Jakobsen,[30] T. Jakoubek,[127] J. Jakubek,[128] D. O. Jamin,[151] D. K. Jana,[79] E. Jansen,[78] R. W. Jansky,[62] J. Janssen,[21] M. Janus,[170] G. Jarlskog,[81] N. Javadov,[65,b] T. Javůrek,[48] L. Jeanty,[15] J. Jejelava,[51a,r] G.-Y. Jeng,[150] D. Jennens,[88] P. Jenni,[48,s] J. Jentzsch,[43] C. Jeske,[170] S. Jézéquel,[5] H. Ji,[173] J. Jia,[148] Y. Jiang,[33b] S. Jiggins,[78] J. Jimenez Pena,[167] S. Jin,[33a] A. Jinaru,[26a] O. Jinnouchi,[157] M. D. Joergensen,[36] P. Johansson,[139] K. A. Johns,[7] K. Jon-And,[146a,146b] G. Jones,[170] R. W. L. Jones,[72] T. J. Jones,[74] J. Jongmanns,[58a] P. M. Jorge,[126a,126b] K. D. Joshi,[84] J. Jovicevic,[159a] X. Ju,[173] C. A. Jung,[43] P. Jussel,[62] A. Juste Rozas,[12,o] M. Kaci,[167] A. Kaczmarska,[39] M. Kado,[117] H. Kagan,[111] M. Kagan,[143] S. J. Kahn,[85] E. Kajomovitz,[45] C. W. Kalderon,[120] S. Kama,[40] A. Kamenshchikov,[130] N. Kanaya,[155]

M. Kaneda,[30] S. Kaneti,[28] V. A. Kantserov,[98] J. Kanzaki,[66] B. Kaplan,[110] A. Kapliy,[31] D. Kar,[53] K. Karakostas,[10] A. Karamaoun,[3] N. Karastathis,[10,107] M. J. Kareem,[54] M. Karnevskiy,[83] S. N. Karpov,[65] Z. M. Karpova,[65] K. Karthik,[110] V. Kartvelishvili,[72] A. N. Karyukhin,[130] L. Kashif,[173] R. D. Kass,[111] A. Kastanas,[14] Y. Kataoka,[155] A. Katre,[49] J. Katzy,[42] K. Kawagoe,[70] T. Kawamoto,[155] G. Kawamura,[54] S. Kazama,[155] V. F. Kazanin,[109,c] M. Y. Kazarinov,[65] R. Keeler,[169] R. Kehoe,[40] J. S. Keller,[42] J. J. Kempster,[77] H. Keoshkerian,[84] O. Kepka,[127] B. P. Keršvan,[75] S. Kersten,[175] R. A. Keyes,[87] F. Khalil-zada,[11] H. Khandanyan,[146a,146b] A. Khanov,[114] A. G. Kharlamov,[109,c] T. J. Khoo,[28] V. Khovanskiy,[97] E. Khramov,[65] J. Khubua,[51b,t] H. Y. Kim,[8] H. Kim,[146a,146b] S. H. Kim,[160] Y. Kim,[31] N. Kimura,[154] O. M. Kind,[16] B. T. King,[74] M. King,[167] R. S. B. King,[120] S. B. King,[168] J. Kirk,[131] A. E. Kiryunin,[101] T. Kishimoto,[67] D. Kisielewska,[38a] F. Kiss,[48] K. Kiuchi,[160] O. Kivernyk,[136] E. Kladiva,[144b] M. H. Klein,[35] M. Klein,[74] U. Klein,[74] K. Kleinknecht,[83] P. Klimek,[146a,146b] A. Klimentov,[25] R. Klingenberg,[43] J. A. Klinger,[84] T. Klioutchnikova,[30] E.-E. Kluge,[58a] P. Kluit,[107] S. Kluth,[101] E. Kneringer,[62] E. B. F. G. Knoops,[85] A. Knue,[53] A. Kobayashi,[155] D. Kobayashi,[157] T. Kobayashi,[155] M. Kobel,[44] M. Kocian,[143] P. Kodys,[129] T. Koffas,[29] E. Koffeman,[107] L. A. Kogan,[120] S. Kohlmann,[175] Z. Kohout,[128] T. Kohriki,[66] T. Koi,[143] H. Kolanoski,[16] I. Koletsou,[5] A. A. Komar,[96,*] Y. Komori,[155] T. Kondo,[66] N. Kondrashova,[42] K. Köneke,[48] A. C. König,[106] S. König,[83] T. Kono,[66,u] R. Konoplich,[110,v] N. Konstantinidis,[78] R. Kopeliansky,[152] S. Koperny,[38a] L. Köpke,[83] A. K. Kopp,[48] K. Korcyl,[39] K. Kordas,[154] A. Korn,[78] A. A. Korol,[109,c] I. Korolkov,[12] E. V. Korolkova,[139] O. Kortner,[101] S. Kortner,[101] T. Kosek,[129] V. V. Kostyukhin,[21] V. M. Kotov,[65] A. Kotwal,[45] A. Kourkoumeli-Charalampidi,[154] C. Kourkoumelis,[9] V. Kouskoura,[25] A. Koutsman,[159a] R. Kowalewski,[169] T. Z. Kowalski,[38a] W. Kozanecki,[136] A. S. Kozhin,[130] V. A. Kramarenko,[99] G. Kramberger,[75] D. Krasnopevtsev,[98] M. W. Krasny,[80] A. Krasznahorkay,[30] J. K. Kraus,[21] A. Kravchenko,[25] S. Kreiss,[110] M. Kretz,[58c] J. Kretzschmar,[74] K. Kreutzfeldt,[52] P. Krieger,[158] K. Krizka,[31] K. Kroeninger,[43] H. Kroha,[101] J. Kroll,[122] J. Kroseberg,[21] J. Krstic,[13] U. Kruchonak,[65] H. Krüger,[21] N. Krumnack,[64] Z. V. Krumshteyn,[65] A. Kruse,[173] M. C. Kruse,[45] M. Kruskal,[22] T. Kubota,[88] H. Kucuk,[78] S. Kuday,[4b] S. Kuehn,[48] A. Kugel,[58c] F. Kuger,[174] A. Kuhl,[137] T. Kuhl,[42] V. Kukhtin,[65] Y. Kulchitsky,[92] S. Kuleshov,[32b] M. Kuna,[132a,132b] T. Kunigo,[68] A. Kupco,[127] H. Kurashige,[67] Y. A. Kurochkin,[92] R. Kurumida,[67] V. Kus,[127] E. S. Kuwertz,[169] M. Kuze,[157] J. Kvita,[115] T. Kwan,[169] D. Kyriazopoulos,[139] A. La Rosa,[49] J. L. La Rosa Navarro,[24d] L. La Rotonda,[37a,37b] C. Lacasta,[167] F. Lacava,[132a,132b] J. Lacey,[29] H. Lacker,[16] D. Lacour,[80] V. R. Lacuesta,[167] E. Ladygin,[65] R. Lafaye,[5] B. Laforge,[80] T. Lagouri,[176] S. Lai,[48] L. Lambourne,[78] S. Lammers,[61] C. L. Lampen,[7] W. Lampl,[7] E. Lançon,[136] U. Landgraf,[48] M. P. J. Landon,[76] V. S. Lang,[58a] J. C. Lange,[12] A. J. Lankford,[163] F. Lanni,[25] K. Lantzsch,[30] S. Laplace,[80] C. Lapoire,[30] J. F. Laporte,[136] T. Lari,[91a] F. Lasagni Manghi,[20a,20b] M. Lassnig,[30] P. Laurelli,[47] W. Lavrijsen,[15] A. T. Law,[137] P. Laycock,[74] O. Le Dortz,[80] E. Le Guirriec,[85] E. Le Menedeu,[12] M. LeBlanc,[169] T. LeCompte,[6] F. Ledroit-Guillon,[55] C. A. Lee,[145b] S. C. Lee,[151] L. Lee,[1] G. Lefebvre,[80] M. Lefebvre,[169] F. Legger,[100] C. Leggett,[15] A. Lehan,[74] G. Lehmann Miotto,[30] X. Lei,[7] W. A. Leight,[29] A. Leisos,[154] A. G. Leister,[176] M. A. L. Leite,[24d] R. Leitner,[129] D. Lellouch,[172] B. Lemmer,[54] K. J. C. Leney,[78] T. Lenz,[21] B. Lenzi,[30] R. Leone,[7] S. Leone,[124a,124b] C. Leonidopoulos,[46] S. Leontsinis,[10] C. Leroy,[95] C. G. Lester,[28] M. Levchenko,[123] J. Levêque,[5] D. Levin,[89] L. J. Levinson,[172] M. Levy,[18] A. Lewis,[120] A. M. Leyko,[21] M. Leyton,[41] B. Li,[33b,w] H. Li,[148] H. L. Li,[31] L. Li,[45] L. Li,[33e] S. Li,[45] Y. Li,[33c,x] Z. Liang,[137] H. Liao,[34] B. Liberti,[133a] A. Liblong,[158] P. Lichard,[30] K. Lie,[165] J. Liebal,[21] W. Liebig,[14] C. Limbach,[21] A. Limosani,[150] S. C. Lin,[151,y] T. H. Lin,[83] F. Linde,[107] B. E. Lindquist,[148] J. T. Linnemann,[90] E. Lipeles,[122] A. Lipniacka,[14] M. Lisovyi,[58b] T. M. Liss,[165] D. Lissauer,[25] A. Lister,[168] A. M. Litke,[137] B. Liu,[151,z] D. Liu,[151] J. Liu,[85] J. B. Liu,[33b] K. Liu,[85] L. Liu,[165] M. Liu,[45] M. Liu,[33b] Y. Liu,[33b] M. Livan,[121a,121b] A. Lleres,[55] J. Llorente Merino,[82] S. L. Lloyd,[76] F. Lo Sterzo,[151] E. Lobodzinska,[42] P. Loch,[7] W. S. Lockman,[137] F. K. Loebinger,[84] A. E. Loevschall-Jensen,[36] A. Loginov,[176] T. Lohse,[16] K. Lohwasser,[42] M. Lokajicek,[127] B. A. Long,[22] J. D. Long,[89] R. E. Long,[72] K. A. Looper,[111] L. Lopes,[126a] D. Lopez Mateos,[57] B. Lopez Paredes,[139] I. Lopez Paz,[12] J. Lorenz,[100] N. Lorenzo Martinez,[61] M. Losada,[162] P. Loscutoff,[15] P. J. Lösel,[100] X. Lou,[33a] A. Lounis,[117] J. Love,[6] P. A. Love,[72] N. Lu,[89] H. J. Lubatti,[138] C. Luci,[132a,132b] A. Lucotte,[55] F. Luehring,[61] W. Lukas,[62] L. Luminari,[132a] O. Lundberg,[146a,146b] B. Lund-Jensen,[147] D. Lynn,[25] R. Lysak,[127] E. Lytken,[81] H. Ma,[25] L. L. Ma,[33d] G. Maccarrone,[47] A. Macchiolo,[101] C. M. Macdonald,[139] J. Machado Miguens,[122,126b] D. Macina,[30] D. Madaffari,[85] R. Madar,[34] H. J. Maddocks,[72] W. F. Mader,[44] A. Madsen,[166] S. Maeland,[14] T. Maeno,[25] A. Maevskiy,[99] E. Magradze,[54] K. Mahboubi,[48] J. Mahlstedt,[107] C. Maiani,[136] C. Maidantchik,[24a] A. A. Maier,[101] T. Maier,[100] A. Maio,[126a,126b,126d] S. Majewski,[116] Y. Makida,[66] N. Makovec,[117] B. Malaescu,[80] Pa. Malecki,[39] V. P. Maleev,[123] F. Malek,[55] U. Mallik,[63] D. Malon,[6] C. Malone,[143] S. Maltezos,[10] V. M. Malyshev,[109] S. Malyukov,[30] J. Mamuzic,[42] G. Mancini,[47] B. Mandelli,[30] L. Mandelli,[91a] I. Mandić,[75] R. Mandrysch,[63] J. Maneira,[126a,126b] A. Manfredini,[101] L. Manhaes de Andrade Filho,[24b] J. Manjarres Ramos,[159b] A. Mann,[100] P. M. Manning,[137] A. Manousakis-Katsikakis,[9] B. Mansoulie,[136] R. Mantifel,[87] M. Mantoani,[54] L. Mapelli,[30] L. March,[145c] G. Marchiori,[80] M. Marcisovsky,[127] C. P. Marino,[169] M. Marjanovic,[13] F. Marroquim,[24a] S. P. Marsden,[84] Z. Marshall,[15] L. F. Marti,[17] S. Marti-Garcia,[167] B. Martin,[90] T. A. Martin,[170] V. J. Martin,[46] B. Martin dit Latour,[14] M. Martinez,[12,o] S. Martin-Haugh,[131] V. S. Martoiu,[26a] A. C. Martyniuk,[78] M. Marx,[138] F. Marzano,[132a] A. Marzin,[30] L. Masetti,[83] T. Mashimo,[155] R. Mashinistov,[96] J. Masik,[84] A. L. Maslennikov,[109,c] I. Massa,[20a,20b] L. Massa,[20a,20b] N. Massol,[5] P. Mastrandrea,[148] A. Mastroberardino,[37a,37b] T. Masubuchi,[155] P. Mättig,[175] J. Mattmann,[83] J. Maurer,[26a] S. J. Maxfield,[74] D. A. Maximov,[109,c] R. Mazini,[151] S. M. Mazza,[91a,91b] L. Mazzaferro,[133a,133b] G. Mc Goldrick,[158] S. P. Mc Kee,[89] A. McCarn,[89] R. L. McCarthy,[148] T. G. McCarthy,[29] N. A. McCubbin,[131] K. W. McFarlane,[56,*] J. A. Mcfayden,[78] G. Mchedlidze,[54] S. J. McMahon,[131] R. A. McPherson,[169,k] M. Medinnis,[42] S. Meehan,[145a] S. Mehlhase,[100] A. Mehta,[74] K. Meier,[58a] C. Meineck,[100] B. Meirose,[41]

B. R. Mellado Garcia,[145c] F. Meloni,[17] A. Mengarelli,[20a,20b] S. Menke,[101] E. Meoni,[161] K. M. Mercurio,[57] S. Mergelmeyer,[21] P. Mermod,[49] L. Merola,[104a,104b] C. Meroni,[91a] F. S. Merritt,[31] A. Messina,[132a,132b] J. Metcalfe,[25] A. S. Mete,[163] C. Meyer,[83] C. Meyer,[122] J-P. Meyer,[136] J. Meyer,[107] R. P. Middleton,[131] S. Miglioranzi,[164a,164c] L. Mijović,[21] G. Mikenberg,[172] M. Mikestikova,[127] M. Mikuž,[75] M. Milesi,[88] A. Milic,[30] D. W. Miller,[31] C. Mills,[46] A. Milov,[172] D. A. Milstead,[146a,146b] A. A. Minaenko,[130] Y. Minami,[155] I. A. Minashvili,[65] A. I. Mincer,[110] B. Mindur,[38a] M. Mineev,[65] Y. Ming,[173] L. M. Mir,[12] T. Mitani,[171] J. Mitrevski,[100] V. A. Mitsou,[167] A. Miucci,[49] P. S. Miyagawa,[139] J. U. Mjörnmark,[81] T. Moa,[146a,146b] K. Mochizuki,[85] S. Mohapatra,[35] W. Mohr,[48] S. Molander,[146a,146b] R. Moles-Valls,[167] K. Mönig,[42] C. Monini,[55] J. Monk,[36] E. Monnier,[85] J. Montejo Berlingen,[12] F. Monticelli,[71] S. Monzani,[132a,132b] R. W. Moore,[3] N. Morange,[117] D. Moreno,[162] M. Moreno Llácer,[54] P. Morettini,[50a] M. Morgenstern,[44] M. Morii,[57] M. Morinaga,[155] V. Morisbak,[119] S. Moritz,[83] A. K. Morley,[147] G. Mornacchi,[30] J. D. Morris,[76] S. S. Mortensen,[36] A. Morton,[53] L. Morvaj,[103] M. Mosidze,[51b] J. Moss,[111] K. Motohashi,[157] R. Mount,[143] E. Mountricha,[25] S. V. Mouraviev,[96,*] E. J. W. Moyse,[86] S. Muanza,[85] R. D. Mudd,[18] F. Mueller,[101] J. Mueller,[125] K. Mueller,[21] R. S. P. Mueller,[100] T. Mueller,[28] D. Muenstermann,[49] P. Mullen,[53] Y. Munwes,[153] J. A. Murillo Quijada,[18] W. J. Murray,[170,131] H. Musheghyan,[54] E. Musto,[152] A. G. Myagkov,[130,aa] M. Myska,[128] O. Nackenhorst,[54] J. Nadal,[54] K. Nagai,[120] R. Nagai,[157] Y. Nagai,[85] K. Nagano,[66] A. Nagarkar,[111] Y. Nagasaka,[59] K. Nagata,[160] M. Nagel,[101] E. Nagy,[85] A. M. Nairz,[30] Y. Nakahama,[30] K. Nakamura,[66] T. Nakamura,[155] I. Nakano,[112] H. Namasivayam,[41] R. F. Naranjo Garcia,[42] R. Narayan,[31] T. Naumann,[42] G. Navarro,[162] R. Nayyar,[7] H. A. Neal,[89] P. Yu. Nechaeva,[96] T. J. Neep,[84] P. D. Nef,[143] A. Negri,[121a,121b] M. Negrini,[20a] S. Nektarijevic,[106] C. Nellist,[117] A. Nelson,[163] S. Nemecek,[127] P. Nemethy,[110] A. A. Nepomuceno,[24a] M. Nessi,[30,ab] M. S. Neubauer,[165] M. Neumann,[175] R. M. Neves,[110] P. Nevski,[25] P. R. Newman,[18] D. H. Nguyen,[6] R. B. Nickerson,[120] R. Nicolaidou,[136] B. Nicquevert,[30] J. Nielsen,[137] N. Nikiforou,[35] A. Nikiforov,[16] V. Nikolaenko,[130,aa] I. Nikolic-Audit,[80] K. Nikolopoulos,[18] J. K. Nilsen,[119] P. Nilsson,[25] Y. Ninomiya,[155] A. Nisati,[132a] R. Nisius,[101] T. Nobe,[157] M. Nomachi,[118] I. Nomidis,[29] T. Nooney,[76] S. Norberg,[113] M. Nordberg,[30] O. Novgorodova,[44] S. Nowak,[101] M. Nozaki,[66] L. Nozka,[115] K. Ntekas,[10] G. Nunes Hanninger,[88] T. Nunnemann,[100] E. Nurse,[78] F. Nuti,[88] B. J. O'Brien,[46] F. O'grady,[7] D. C. O'Neil,[142] V. O'Shea,[53] F. G. Oakham,[29,d] H. Oberlack,[101] T. Obermann,[21] J. Ocariz,[80] A. Ochi,[67] I. Ochoa,[78] J. P. Ochoa-Ricoux,[32a] S. Oda,[70] S. Odaka,[66] H. Ogren,[61] A. Oh,[84] S. H. Oh,[45] C. C. Ohm,[15] H. Ohman,[166] H. Oide,[30] W. Okamura,[118] H. Okawa,[160] Y. Okumura,[31] T. Okuyama,[155] A. Olariu,[26a] S. A. Olivares Pino,[46] D. Oliveira Damazio,[25] E. Oliver Garcia,[167] A. Olszewski,[39] J. Olszowska,[39] A. Onofre,[126a,126e] P. U. E. Onyisi,[31,q] C. J. Oram,[159a] M. J. Oreglia,[31] Y. Oren,[153] D. Orestano,[134a,134b] N. Orlando,[154] C. Oropeza Barrera,[53] R. S. Orr,[158] B. Osculati,[50a,50b] R. Ospanov,[84] G. Otero y Garzon,[27] H. Otono,[70] M. Ouchrif,[135d] E. A. Ouellette,[169] F. Ould-Saada,[119] A. Ouraou,[136] K. P. Oussoren,[107] Q. Ouyang,[33a] A. Ovcharova,[15] M. Owen,[53] R. E. Owen,[18] V. E. Ozcan,[19a] N. Ozturk,[8] K. Pachal,[142] A. Pacheco Pages,[12] C. Padilla Aranda,[12] M. Pagáčová,[48] S. Pagan Griso,[15] E. Paganis,[139] C. Pahl,[101] F. Paige,[25] P. Pais,[86] K. Pajchel,[119] G. Palacino,[159b] S. Palestini,[30] M. Palka,[38b] D. Pallin,[34] A. Palma,[126a,126b] Y. B. Pan,[173] E. Panagiotopoulou,[10] C. E. Pandini,[80] J. G. Panduro Vazquez,[77] P. Pani,[146a,146b] S. Panitkin,[25] D. Pantea,[26a] L. Paolozzi,[49] Th. D. Papadopoulou,[10] K. Papageorgiou,[154] A. Paramonov,[6] D. Paredes Hernandez,[154] M. A. Parker,[28] K. A. Parker,[139] F. Parodi,[50a,50b] J. A. Parsons,[35] U. Parzefall,[48] E. Pasqualucci,[132a] S. Passaggio,[50a] F. Pastore,[134a,134b,*] Fr. Pastore,[77] G. Pásztor,[29] S. Pataraia,[175] N. D. Patel,[150] J. R. Pater,[84] T. Pauly,[30] J. Pearce,[169] B. Pearson,[113] L. E. Pedersen,[36] M. Pedersen,[119] S. Pedraza Lopez,[167] R. Pedro,[126a,126b] S. V. Peleganchuk,[109] D. Pelikan,[166] H. Peng,[33b] B. Penning,[31] J. Penwell,[61] D. V. Perepelitsa,[25] E. Perez Codina,[159a] M. T. Pérez García-Estañ,[167] L. Perini,[91a,91b] H. Pernegger,[30] S. Perrella,[104a,104b] R. Peschke,[42] V. D. Peshekhonov,[65] K. Peters,[30] R. F. Y. Peters,[84] B. A. Petersen,[30] T. C. Petersen,[36] E. Petit,[42] A. Petridis,[146a,146b] C. Petridou,[154] E. Petrolo,[132a] F. Petrucci,[134a,134b] N. E. Pettersson,[157] R. Pezoa,[32b] P. W. Phillips,[131] G. Piacquadio,[143] E. Pianori,[170] A. Picazio,[49] E. Piccaro,[76] M. Piccinini,[20a,20b] M. A. Pickering,[120] R. Piegaia,[27] D. T. Pignotti,[111] J. E. Pilcher,[31] A. D. Pilkington,[84] J. Pina,[126a,126b,126d] M. Pinamonti,[164a,164c,ac] J. L. Pinfold,[3] A. Pingel,[36] B. Pinto,[126a] S. Pires,[80] M. Pitt,[172] C. Pizio,[91a,91b] L. Plazak,[144a] M.-A. Pleier,[25] V. Pleskot,[129] E. Plotnikova,[65] P. Plucinski,[146a,146b] D. Pluth,[64] R. Poettgen,[83] L. Poggioli,[117] D. Pohl,[21] G. Polesello,[121a] A. Policicchio,[37a,37b] R. Polifka,[158] A. Polini,[20a] C. S. Pollard,[53] V. Polychronakos,[25] K. Pommès,[30] L. Pontecorvo,[132a] B. G. Pope,[90] G. A. Popeneciu,[26b] D. S. Popovic,[13] A. Poppleton,[30] S. Pospisil,[128] K. Potamianos,[15] I. N. Potrap,[65] C. J. Potter,[149] C. T. Potter,[116] G. Poulard,[30] J. Poveda,[30] V. Pozdnyakov,[65] P. Pralavorio,[85] A. Pranko,[15] S. Prasad,[30] S. Prell,[64] D. Price,[84] L. E. Price,[6] M. Primavera,[73a] S. Prince,[87] M. Proissl,[46] K. Prokofiev,[60c] F. Prokoshin,[32b] E. Protopapadaki,[136] S. Protopopescu,[25] J. Proudfoot,[6] M. Przybycien,[38a] E. Ptacek,[116] D. Puddu,[134a,134b] E. Pueschel,[86] D. Puldon,[148] M. Purohit,[25,ad] P. Puzo,[117] J. Qian,[89] G. Qin,[53] Y. Qin,[84] A. Quadt,[54] D. R. Quarrie,[15] W. B. Quayle,[164a,164b] M. Queitsch-Maitland,[84] D. Quilty,[53] S. Raddum,[119] V. Radeka,[25] V. Radescu,[42] S. K. Radhakrishnan,[148] P. Radloff,[116] P. Rados,[88] F. Ragusa,[91a,91b] G. Rahal,[178] S. Rajagopalan,[25] M. Rammensee,[30] C. Rangel-Smith,[166] F. Rauscher,[100] S. Rave,[83] T. Ravenscroft,[53] M. Raymond,[30] A. L. Read,[119] N. P. Readioff,[74] D. M. Rebuzzi,[121a,121b] A. Redelbach,[174] G. Redlinger,[25] R. Reece,[137] K. Reeves,[41] L. Rehnisch,[16] H. Reisin,[27] M. Relich,[163] C. Rembser,[30] H. Ren,[33a] A. Renaud,[117] M. Rescigno,[132a] S. Resconi,[91a] O. L. Rezanova,[109,c] P. Reznicek,[129] R. Rezvani,[95] R. Richter,[101] S. Richter,[78] E. Richter-Was,[38b] O. Ricken,[21] M. Ridel,[80] P. Rieck,[16] C. J. Riegel,[175] J. Rieger,[54] M. Rijssenbeek,[148] A. Rimoldi,[121a,121b] L. Rinaldi,[20a] B. Ristić,[49] E. Ritsch,[62] I. Riu,[12] F. Rizatdinova,[114] E. Rizvi,[76] S. H. Robertson,[87,k] A. Robichaud-Veronneau,[87] D. Robinson,[28] J. E. M. Robinson,[84] A. Robson,[53] C. Roda,[124a,124b] S. Roe,[30] O. Røhne,[119] S. Rolli,[161] A. Romaniouk,[98] M. Romano,[20a,20b] S. M. Romano Saez,[34] E. Romero Adam,[167] N. Rompotis,[138] M. Ronzani,[48] L. Roos,[80] E. Ros,[167] S. Rosati,[132a] K. Rosbach,[48] P. Rose,[137] P. L. Rosendahl,[14] O. Rosenthal,[141]

V. Rossetti,[146a,146b] E. Rossi,[104a,104b] L. P. Rossi,[50a] R. Rosten,[138] M. Rotaru,[26a] I. Roth,[172] J. Rothberg,[138] D. Rousseau,[117]
C. R. Royon,[136] A. Rozanov,[85] Y. Rozen,[152] X. Ruan,[145c] F. Rubbo,[143] I. Rubinskiy,[42] V. I. Rud,[99] C. Rudolph,[44]
M. S. Rudolph,[158] F. Rühr,[48] A. Ruiz-Martinez,[30] Z. Rurikova,[48] N. A. Rusakovich,[65] A. Ruschke,[100] H. L. Russell,[138]
J. P. Rutherfoord,[7] N. Ruthmann,[48] Y. F. Ryabov,[123] M. Rybar,[129] G. Rybkin,[117] N. C. Ryder,[120] A. F. Saavedra,[150]
G. Sabato,[107] S. Sacerdoti,[27] A. Saddique,[3] H. F-W. Sadrozinski,[137] R. Sadykov,[65] F. Safai Tehrani,[132a] M. Saimpert,[136]
H. Sakamoto,[155] Y. Sakurai,[171] G. Salamanna,[134a,134b] A. Salamon,[133a] M. Saleem,[113] D. Salek,[107] P. H. Sales De Bruin,[138]
D. Salihagic,[101] A. Salnikov,[143] J. Salt,[167] D. Salvatore,[37a,37b] F. Salvatore,[149] A. Salvucci,[106] A. Salzburger,[30]
D. Sampsonidis,[154] A. Sanchez,[104a,104b] J. Sánchez,[167] V. Sanchez Martinez,[167] H. Sandaker,[14] R. L. Sandbach,[76]
H. G. Sander,[83] M. P. Sanders,[100] M. Sandhoff,[175] C. Sandoval,[162] R. Sandstroem,[101] D. P. C. Sankey,[131] M. Sannino,[50a,50b]
A. Sansoni,[47] C. Santoni,[34] R. Santonico,[133a,133b] H. Santos,[126a] I. Santoyo Castillo,[149] K. Sapp,[125] A. Sapronov,[65]
J. G. Saraiva,[126a,126d] B. Sarrazin,[21] O. Sasaki,[66] Y. Sasaki,[155] K. Sato,[160] G. Sauvage,[5,*] E. Sauvan,[5] G. Savage,[77] P. Savard,[158,d]
C. Sawyer,[120] L. Sawyer,[79,n] J. Saxon,[31] C. Sbarra,[20a] A. Sbrizzi,[20a,20b] T. Scanlon,[78] D. A. Scannicchio,[163] M. Scarcella,[150]
V. Scarfone,[37a,37b] J. Schaarschmidt,[172] P. Schacht,[101] D. Schaefer,[30] R. Schaefer,[42] J. Schaeffer,[83] S. Schaepe,[21] S. Schaetzel,[58b]
U. Schäfer,[83] A. C. Schaffer,[117] D. Schaile,[100] R. D. Schamberger,[148] V. Scharf,[58a] V. A. Schegelsky,[123] D. Scheirich,[129]
M. Schernau,[163] C. Schiavi,[50a,50b] C. Schillo,[48] M. Schioppa,[37a,37b] S. Schlenker,[30] E. Schmidt,[48] K. Schmieden,[30] C. Schmitt,[83]
S. Schmitt,[58b] S. Schmitt,[42] B. Schneider,[159a] Y. J. Schnellbach,[74] U. Schnoor,[44] L. Schoeffel,[136] A. Schoening,[58b]
B. D. Schoenrock,[90] E. Schopf,[21] A. L. S. Schorlemmer,[54] M. Schott,[83] D. Schouten,[159a] J. Schovancova,[8] S. Schramm,[158]
M. Schreyer,[174] C. Schroeder,[83] N. Schuh,[83] M. J. Schultens,[21] H.-C. Schultz-Coulon,[58a] H. Schulz,[16] M. Schumacher,[48]
B. A. Schumm,[137] Ph. Schune,[136] C. Schwanenberger,[84] A. Schwartzman,[143] T. A. Schwarz,[89] Ph. Schwegler,[101]
Ph. Schwemling,[136] R. Schwienhorst,[90] J. Schwindling,[136] T. Schwindt,[21] M. Schwoerer,[5] F. G. Sciacca,[17] E. Scifo,[117]
G. Sciolla,[23] F. Scuri,[124a,124b] F. Scutti,[21] J. Searcy,[89] G. Sedov,[42] E. Sedykh,[123] P. Seema,[21] S. C. Seidel,[105] A. Seiden,[137]
F. Seifert,[128] J. M. Seixas,[24a] G. Sekhniaidze,[104a] K. Sekhon,[89] S. J. Sekula,[40] K. E. Selbach,[46] D. M. Seliverstov,[123,*]
N. Semprini-Cesari,[20a,20b] C. Serfon,[30] L. Serin,[117] L. Serkin,[164a,164b] T. Serre,[85] M. Sessa,[134a,134b] R. Seuster,[159a] H. Severini,[113]
T. Sfiligoj,[75] F. Sforza,[101] A. Sfyrla,[30] E. Shabalina,[54] M. Shamim,[116] L. Y. Shan,[33a] R. Shang,[165] J. T. Shank,[22] M. Shapiro,[15]
P. B. Shatalov,[97] K. Shaw,[164a,164b] S. M. Shaw,[84] A. Shcherbakova,[146a,146b] C. Y. Shehu,[149] P. Sherwood,[78] L. Shi,[151,ae]
S. Shimizu,[67] C. O. Shimmin,[163] M. Shimojima,[102] M. Shiyakova,[65] A. Shmeleva,[96] D. Shoaleh Saadi,[95] M. J. Shochet,[31]
S. Shojaii,[91a,91b] S. Shrestha,[111] E. Shulga,[98] M. A. Shupe,[7] S. Shushkevich,[42] P. Sicho,[127] O. Sidiropoulou,[174] D. Sidorov,[114]
A. Sidoti,[20a,20b] F. Siegert,[44] Dj. Sijacki,[13] J. Silva,[126a,126d] Y. Silver,[153] S. B. Silverstein,[146a] V. Simak,[128] O. Simard,[5]
Lj. Simic,[13] S. Simion,[117] E. Simioni,[83] B. Simmons,[78] D. Simon,[34] R. Simoniello,[91a,91b] P. Sinervo,[158] N. B. Sinev,[116]
G. Siragusa,[174] A. N. Sisakyan,[65,*] S. Yu. Sivoklokov,[99] J. Sjölin,[146a,146b] T. B. Sjursen,[14] M. B. Skinner,[72] H. P. Skottowe,[57]
P. Skubic,[113] M. Slater,[18] T. Slavicek,[128] M. Slawinska,[107] K. Sliwa,[161] V. Smakhtin,[172] B. H. Smart,[46] L. Smestad,[14]
S. Yu. Smirnov,[98] Y. Smirnov,[98] L. N. Smirnova,[99,af] O. Smirnova,[81] M. N. K. Smith,[35] M. Smizanska,[72] K. Smolek,[128]
A. A. Snesarev,[96] G. Snidero,[76] S. Snyder,[25] R. Sobie,[169,k] F. Socher,[44] A. Soffer,[153] D. A. Soh,[151,ae] C. A. Solans,[30]
M. Solar,[128] J. Solc,[128] E. Yu. Soldatov,[98] U. Soldevila,[167] A. A. Solodkov,[130] A. Soloshenko,[65] O. V. Solovyanov,[130]
V. Solovyev,[123] P. Sommer,[48] H. Y. Song,[33b] N. Soni,[1] A. Sood,[15] A. Sopczak,[128] B. Sopko,[128] V. Sopko,[128] V. Sorin,[12]
D. Sosa,[58b] M. Sosebee,[8] C. L. Sotiropoulou,[124a,124b] R. Soualah,[164a,164c] P. Soueid,[95] A. M. Soukharev,[109,c] D. South,[42]
S. Spagnolo,[73a,73b] M. Spalla,[124a,124b] F. Spanò,[77] W. R. Spearman,[57] F. Spettel,[101] R. Spighi,[20a] G. Spigo,[30] L. A. Spiller,[88]
M. Spousta,[129] T. Spreitzer,[158] R. D. St. Denis,[53,*] S. Staerz,[44] J. Stahlman,[122] R. Stamen,[58a] S. Stamm,[16] E. Stanecka,[39]
C. Stanescu,[134a] M. Stanescu-Bellu,[42] M. M. Stanitzki,[42] S. Stapnes,[119] E. A. Starchenko,[130] J. Stark,[55] P. Staroba,[127]
P. Starovoitov,[42] R. Staszewski,[39] P. Stavina,[144a,*] P. Steinberg,[25] B. Stelzer,[142] H. J. Stelzer,[30] O. Stelzer-Chilton,[159a]
H. Stenzel,[52] S. Stern,[101] G. A. Stewart,[53] J. A. Stillings,[21] M. C. Stockton,[87] M. Stoebe,[87] G. Stoicea,[26a] P. Stolte,[54]
S. Stonjek,[101] A. R. Stradling,[8] A. Straessner,[44] M. E. Stramaglia,[17] J. Strandberg,[147] S. Strandberg,[146a,146b] A. Strandlie,[119]
E. Strauss,[143] M. Strauss,[113] P. Strizenec,[144b] R. Ströhmer,[174] D. M. Strom,[116] R. Stroynowski,[40] A. Strubig,[106] S. A. Stucci,[17]
B. Stugu,[14] N. A. Styles,[42] D. Su,[143] J. Su,[125] R. Subramaniam,[79] A. Succurro,[12] Y. Sugaya,[118] C. Suhr,[108] M. Suk,[128]
V. V. Sulin,[96] S. Sultansoy,[4c] T. Sumida,[68] S. Sun,[57] X. Sun,[33a] J. E. Sundermann,[48] K. Suruliz,[149] G. Susinno,[37a,37b]
M. R. Sutton,[149] S. Suzuki,[66] Y. Suzuki,[66] M. Svatos,[127] S. Swedish,[168] M. Swiatlowski,[143] I. Sykora,[144a] T. Sykora,[129] D. Ta,[90]
C. Taccini,[134a,134b] K. Tackmann,[42] J. Taenzer,[158] A. Taffard,[163] R. Tafirout,[159a] N. Taiblum,[153] H. Takai,[25] R. Takashima,[69]
H. Takeda,[67] T. Takeshita,[140] Y. Takubo,[66] M. Talby,[85] A. A. Talyshev,[109,c] J. Y. C. Tam,[174] K. G. Tan,[88] J. Tanaka,[155]
R. Tanaka,[117] S. Tanaka,[66] B. B. Tannenwald,[111] N. Tannoury,[21] S. Tapprogge,[83] S. Tarem,[152] F. Tarrade,[29] G. F. Tartarelli,[91a]
P. Tas,[129] M. Tasevsky,[127] T. Tashiro,[68] E. Tassi,[37a,37b] A. Tavares Delgado,[126a,126b] Y. Tayalati,[135d] F. E. Taylor,[94]
G. N. Taylor,[88] W. Taylor,[159b] F. A. Teischinger,[30] M. Teixeira Dias Castanheira,[76] P. Teixeira-Dias,[77] K. K. Temming,[48]
H. Ten Kate,[30] P. K. Teng,[151] J. J. Teoh,[118] F. Tepel,[175] S. Terada,[66] K. Terashi,[155] J. Terron,[82] S. Terzo,[101] M. Testa,[47]
R. J. Teuscher,[158,k] J. Therhaag,[21] T. Theveneaux-Pelzer,[34] J. P. Thomas,[18] J. Thomas-Wilsker,[77] E. N. Thompson,[35]
P. D. Thompson,[18] R. J. Thompson,[84] A. S. Thompson,[53] L. A. Thomsen,[36] E. Thomson,[122] M. Thomson,[28] R. P. Thun,[89,*]
M. J. Tibbetts,[15] R. E. Ticse Torres,[85] V. O. Tikhomirov,[96,ag] Yu. A. Tikhonov,[109,c] S. Timoshenko,[98] E. Tiouchichine,[85]
P. Tipton,[176] S. Tisserant,[85] T. Todorov,[5,*] S. Todorova-Nova,[129] J. Tojo,[70] S. Tokár,[144a] K. Tokushuku,[66] K. Tollefson,[90]
E. Tolley,[57] L. Tomlinson,[84] M. Tomoto,[103] L. Tompkins,[143,ah] K. Toms,[105] E. Torrence,[116] H. Torres,[142] E. Torró Pastor,[167]
J. Toth,[85,ai] F. Touchard,[85] D. R. Tovey,[139] T. Trefzger,[174] L. Tremblet,[30] A. Tricoli,[30] I. M. Trigger,[159a] S. Trincaz-Duvoid,[80]

M. F. Tripiana,[12] W. Trischuk,[158] B. Trocmé,[55] C. Troncon,[91a] M. Trottier-McDonald,[15] M. Trovatelli,[134a,134b] P. True,[90] L. Truong,[164a,164c] M. Trzebinski,[39] A. Trzupek,[39] C. Tsarouchas,[30] J. C-L. Tseng,[120] P. V. Tsiareshka,[92] D. Tsionou,[154] G. Tsipolitis,[10] N. Tsirintanis,[9] S. Tsiskaridze,[12] V. Tsiskaridze,[48] E. G. Tskhadadze,[51a] I. I. Tsukerman,[97] V. Tsulaia,[15] S. Tsuno,[66] D. Tsybychev,[148] A. Tudorache,[26a] V. Tudorache,[26a] A. N. Tuna,[122] S. A. Tupputi,[20a,20b] S. Turchikhin,[99,af] D. Turecek,[128] R. Turra,[91a,91b] A. J. Turvey,[40] P. M. Tuts,[35] A. Tykhonov,[49] M. Tylmad,[146a,146b] M. Tyndel,[131] I. Ueda,[155] R. Ueno,[29] M. Ughetto,[146a,146b] M. Ugland,[14] M. Uhlenbrock,[21] F. Ukegawa,[160] G. Unal,[30] A. Undrus,[25] G. Unel,[163] F. C. Ungaro,[48] Y. Unno,[66] C. Unverdorben,[100] J. Urban,[144b] P. Urquijo,[88] P. Urrejola,[83] G. Usai,[8] A. Usanova,[62] L. Vacavant,[85] V. Vacek,[128] B. Vachon,[87] C. Valderanis,[83] N. Valencic,[107] S. Valentinetti,[20a,20b] A. Valero,[167] L. Valery,[12] S. Valkar,[129] E. Valladolid Gallego,[167] S. Vallecorsa,[49] J. A. Valls Ferrer,[167] W. Van Den Wollenberg,[107] P. C. Van Der Deijl,[107] R. van der Geer,[107] H. van der Graaf,[107] R. Van Der Leeuw,[107] N. van Eldik,[152] P. van Gemmeren,[6] J. Van Nieuwkoop,[142] I. van Vulpen,[107] M. C. van Woerden,[30] M. Vanadia,[132a,132b] W. Vandelli,[30] R. Vanguri,[122] A. Vaniachine,[6] F. Vannucci,[80] G. Vardanyan,[177] R. Vari,[132a] E. W. Varnes,[7] T. Varol,[40] D. Varouchas,[80] A. Vartapetian,[8] K. E. Varvell,[150] F. Vazeille,[34] T. Vazquez Schroeder,[87] J. Veatch,[7] F. Veloso,[126a,126c] T. Velz,[21] S. Veneziano,[132a] A. Ventura,[73a,73b] D. Ventura,[86] M. Venturi,[169] N. Venturi,[158] A. Venturini,[23] V. Vercesi,[121a] M. Verducci,[132a,132b] W. Verkerke,[107] J. C. Vermeulen,[107] A. Vest,[44] M. C. Vetterli,[142,d] O. Viazlo,[81] I. Vichou,[165] T. Vickey,[139] O. E. Vickey Boeriu,[139] G. H. A. Viehhauser,[120] S. Viel,[15] R. Vigne,[30] M. Villa,[20a,20b] M. Villaplana Perez,[91a,91b] E. Vilucchi,[47] M. G. Vincter,[29] V. B. Vinogradov,[65] I. Vivarelli,[149] F. Vives Vaque,[3] S. Vlachos,[10] D. Vladoiu,[100] M. Vlasak,[128] M. Vogel,[32a] P. Vokac,[128] G. Volpi,[124a,124b] M. Volpi,[88] H. von der Schmitt,[101] H. von Radziewski,[48] E. von Toerne,[21] V. Vorobel,[129] K. Vorobev,[98] M. Vos,[167] R. Voss,[30] J. H. Vossebeld,[74] N. Vranjes,[13] M. Vranjes Milosavljevic,[13] V. Vrba,[127] M. Vreeswijk,[107] R. Vuillermet,[30] I. Vukotic,[31] Z. Vykydal,[128] P. Wagner,[21] W. Wagner,[175] H. Wahlberg,[71] S. Wahrmund,[44] J. Wakabayashi,[103] J. Walder,[72] R. Walker,[100] W. Walkowiak,[141] C. Wang,[33c] F. Wang,[173] H. Wang,[15] H. Wang,[40] J. Wang,[42] J. Wang,[33a] K. Wang,[87] R. Wang,[6] S. M. Wang,[151] T. Wang,[21] X. Wang,[176] C. Wanotayaroj,[116] A. Warburton,[87] C. P. Ward,[28] D. R. Wardrope,[78] M. Warsinsky,[48] A. Washbrook,[46] C. Wasicki,[42] P. M. Watkins,[18] A. T. Watson,[18] I. J. Watson,[150] M. F. Watson,[18] G. Watts,[138] S. Watts,[84] B. M. Waugh,[78] S. Webb,[84] M. S. Weber,[17] S. W. Weber,[174] J. S. Webster,[31] A. R. Weidberg,[120] B. Weinert,[61] J. Weingarten,[54] C. Weiser,[48] H. Weits,[107] P. S. Wells,[30] T. Wenaus,[25] T. Wengler,[30] S. Wenig,[30] N. Wermes,[21] M. Werner,[48] P. Werner,[30] M. Wessels,[58a] J. Wetter,[161] K. Whalen,[29] A. M. Wharton,[72] A. White,[8] M. J. White,[1] R. White,[32b] S. White,[124a,124b] D. Whiteson,[163] F. J. Wickens,[131] W. Wiedenmann,[173] M. Wielers,[131] P. Wienemann,[21] C. Wiglesworth,[36] L. A. M. Wiik-Fuchs,[21] A. Wildauer,[101] H. G. Wilkens,[30] H. H. Williams,[122] S. Williams,[107] C. Willis,[90] S. Willocq,[86] A. Wilson,[89] J. A. Wilson,[18] I. Wingerter-Seez,[5] F. Winklmeier,[116] B. T. Winter,[21] M. Wittgen,[143] J. Wittkowski,[100] S. J. Wollstadt,[83] M. W. Wolter,[39] H. Wolters,[126a,126c] B. K. Wosiek,[39] J. Wotschack,[30] M. J. Woudstra,[84] K. W. Wozniak,[39] M. Wu,[55] M. Wu,[31] S. L. Wu,[173] X. Wu,[49] Y. Wu,[89] T. R. Wyatt,[84] B. M. Wynne,[46] S. Xella,[36] D. Xu,[33a] L. Xu,[33b,aj] B. Yabsley,[150] S. Yacoob,[145b,ak] R. Yakabe,[67] M. Yamada,[66] Y. Yamaguchi,[118] A. Yamamoto,[66] S. Yamamoto,[155] T. Yamanaka,[155] K. Yamauchi,[103] Y. Yamazaki,[67] Z. Yan,[22] H. Yang,[33e] H. Yang,[173] Y. Yang,[151] L. Yao,[33a] W-M. Yao,[15] Y. Yasu,[66] E. Yatsenko,[5] K. H. Yau Wong,[21] J. Ye,[40] S. Ye,[25] I. Yeletskikh,[65] A. L. Yen,[57] E. Yildirim,[42] K. Yorita,[171] R. Yoshida,[6] K. Yoshihara,[122] C. Young,[143] C. J. S. Young,[30] S. Youssef,[22] D. R. Yu,[15] J. Yu,[8] J. M. Yu,[89] J. Yu,[114] L. Yuan,[67] A. Yurkewicz,[108] I. Yusuff,[28,al] B. Zabinski,[39] R. Zaidan,[63] A. M. Zaitsev,[130,aa] J. Zalieckas,[14] A. Zaman,[148] S. Zambito,[57] L. Zanello,[132a,132b] D. Zanzi,[88] C. Zeitnitz,[175] M. Zeman,[128] A. Zemla,[38a] K. Zengel,[23] O. Zenin,[130] T. Ženiš,[144a] D. Zerwas,[117] D. Zhang,[89] F. Zhang,[173] J. Zhang,[6] L. Zhang,[48] R. Zhang,[33b] X. Zhang,[33d] Z. Zhang,[117] X. Zhao,[40] Y. Zhao,[33d,117] Z. Zhao,[33b] A. Zhemchugov,[65] J. Zhong,[120] B. Zhou,[89] C. Zhou,[45] L. Zhou,[35] L. Zhou,[40] N. Zhou,[163] C. G. Zhu,[33d] H. Zhu,[33a] J. Zhu,[89] Y. Zhu,[33b] X. Zhuang,[33a] K. Zhukov,[96] A. Zibell,[174] D. Zieminska,[61] N. I. Zimine,[65] C. Zimmermann,[83] S. Zimmermann,[48] Z. Zinonos,[54] M. Zinser,[83] M. Ziolkowski,[141] L. Živković,[13] G. Zobernig,[173] A. Zoccoli,[20a,20b] M. zur Nedden,[16] G. Zurzolo,[104a,104b] and L. Zwalinski[30]

(ATLAS Collaboration)

[1]*Department of Physics, University of Adelaide, Adelaide, Australia*
[2]*Physics Department, SUNY Albany, Albany, New York, USA*
[3]*Department of Physics, University of Alberta, Edmonton, Alberta, Canada*
[4a]*Department of Physics, Ankara University, Ankara, Turkey*
[4b]*Istanbul Aydin University, Istanbul, Turkey*
[4c]*Division of Physics, TOBB University of Economics and Technology, Ankara, Turkey*
[5]*LAPP, CNRS/IN2P3 and Université Savoie Mont Blanc, Annecy-le-Vieux, France*
[6]*High Energy Physics Division, Argonne National Laboratory, Argonne, Illinois, USA*
[7]*Department of Physics, University of Arizona, Tucson, Arizona, USA*
[8]*Department of Physics, The University of Texas at Arlington, Arlington, Texas, USA*
[9]*Physics Department, University of Athens, Athens, Greece*
[10]*Physics Department, National Technical University of Athens, Zografou, Greece*
[11]*Institute of Physics, Azerbaijan Academy of Sciences, Baku, Azerbaijan*
[12]*Institut de Física d'Altes Energies and Departament de Física de la Universitat Autònoma de Barcelona, Barcelona, Spain*

[13]*Institute of Physics, University of Belgrade, Belgrade, Serbia*

[14]*Department for Physics and Technology, University of Bergen, Bergen, Norway*

[15]*Physics Division, Lawrence Berkeley National Laboratory and University of California, Berkeley, California, USA*

[16]*Department of Physics, Humboldt University, Berlin, Germany*

[17]*Albert Einstein Center for Fundamental Physics and Laboratory for High Energy Physics, University of Bern, Bern, Switzerland*

[18]*School of Physics and Astronomy, University of Birmingham, Birmingham, United Kingdom*

[19a]*Department of Physics, Bogazici University, Istanbul, Turkey*

[19b]*Department of Physics, Dogus University, Istanbul, Turkey*

[19c]*Department of Physics Engineering, Gaziantep University, Gaziantep, Turkey*

[20a]*INFN Sezione di Bologna, Bologna, Italy*

[20b]*Dipartimento di Fisica e Astronomia, Università di Bologna, Bologna, Italy*

[21]*Physikalisches Institut, University of Bonn, Bonn, Germany*

[22]*Department of Physics, Boston University, Boston, Massachusetts, USA*

[23]*Department of Physics, Brandeis University, Waltham, Massachusetts, USA*

[24a]*Universidade Federal do Rio De Janeiro COPPE/EE/IF, Rio de Janeiro, Brazil*

[24b]*Electrical Circuits Department, Federal University of Juiz de Fora (UFJF), Juiz de Fora, Brazil*

[24c]*Federal University of Sao Joao del Rei (UFSJ), Sao Joao del Rei, Brazil*

[24d]*Instituto de Fisica, Universidade de Sao Paulo, Sao Paulo, Brazil*

[25]*Physics Department, Brookhaven National Laboratory, Upton, New York, USA*

[26a]*National Institute of Physics and Nuclear Engineering, Bucharest, Romania*

[26b]*National Institute for Research and Development of Isotopic and Molecular Technologies, Physics Department, Cluj Napoca, Romania*

[26c]*University Politehnica Bucharest, Bucharest, Romania*

[26d]*West University in Timisoara, Timisoara, Romania*

[27]*Departamento de Física, Universidad de Buenos Aires, Buenos Aires, Argentina*

[28]*Cavendish Laboratory, University of Cambridge, Cambridge, United Kingdom*

[29]*Department of Physics, Carleton University, Ottawa, Ontario, Canada*

[30]*CERN, Geneva, Switzerland*

[31]*Enrico Fermi Institute, University of Chicago, Chicago, Illinois, USA*

[32a]*Departamento de Física, Pontificia Universidad Católica de Chile, Santiago, Chile*

[32b]*Departamento de Física, Universidad Técnica Federico Santa María, Valparaíso, Chile*

[33a]*Institute of High Energy Physics, Chinese Academy of Sciences, Beijing, China*

[33b]*Department of Modern Physics, University of Science and Technology of China, Anhui, China*

[33c]*Department of Physics, Nanjing University, Jiangsu, China*

[33d]*School of Physics, Shandong University, Shandong, China*

[33e]*Department of Physics and Astronomy, Shanghai Key Laboratory for Particle Physics and Cosmology, Shanghai Jiao Tong University, Shanghai, China*

[33f]*Physics Department, Tsinghua University, Beijing 100084, China*

[34]*Laboratoire de Physique Corpusculaire, Clermont Université and Université Blaise Pascal and CNRS/IN2P3, Clermont-Ferrand, France*

[35]*Nevis Laboratory, Columbia University, Irvington, New York, USA*

[36]*Niels Bohr Institute, University of Copenhagen, Kobenhavn, Denmark*

[37a]*INFN Gruppo Collegato di Cosenza, Laboratori Nazionali di Frascati, Italy*

[37b]*Dipartimento di Fisica, Università della Calabria, Rende, Italy*

[38a]*AGH University of Science and Technology, Faculty of Physics and Applied Computer Science, Krakow, Poland*

[38b]*Marian Smoluchowski Institute of Physics, Jagiellonian University, Krakow, Poland*

[39]*Institute of Nuclear Physics Polish Academy of Sciences, Krakow, Poland*

[40]*Physics Department, Southern Methodist University, Dallas, Texas, USA*

[41]*Physics Department, University of Texas at Dallas, Richardson, Texas, USA*

[42]*DESY, Hamburg and Zeuthen, Germany*

[43]*Institut für Experimentelle Physik IV, Technische Universität Dortmund, Dortmund, Germany*

[44]*Institut für Kern- und Teilchenphysik, Technische Universität Dresden, Dresden, Germany*

[45]*Department of Physics, Duke University, Durham, North Carolina, USA*

[46]*SUPA - School of Physics and Astronomy, University of Edinburgh, Edinburgh, United Kingdom*

[47]*INFN Laboratori Nazionali di Frascati, Frascati, Italy*

[48]*Fakultät für Mathematik und Physik, Albert-Ludwigs-Universität, Freiburg, Germany*

[49]*Section de Physique, Université de Genève, Geneva, Switzerland*

[50a]*INFN Sezione di Genova, Italy*

[50b]*Dipartimento di Fisica, Università di Genova, Genova, Italy*

[51a]*E. Andronikashvili Institute of Physics, Iv. Javakhishvili Tbilisi State University, Tbilisi, Georgia*

[51b]*High Energy Physics Institute, Tbilisi State University, Tbilisi, Georgia*

[52]*II Physikalisches Institut, Justus-Liebig-Universität Giessen, Giessen, Germany*

[53]*SUPA - School of Physics and Astronomy, University of Glasgow, Glasgow, United Kingdom*

[54]*II Physikalisches Institut, Georg-August-Universität, Göttingen, Germany*

[55]*Laboratoire de Physique Subatomique et de Cosmologie, Université Grenoble-Alpes, CNRS/IN2P3, Grenoble, France*

[56]*Department of Physics, Hampton University, Hampton, Virginia, USA*

[57]*Laboratory for Particle Physics and Cosmology, Harvard University, Cambridge, Massachusetts, USA*

[58a]*Kirchhoff-Institut für Physik, Ruprecht-Karls-Universität Heidelberg, Heidelberg, Germany*

[58b]*Physikalisches Institut, Ruprecht-Karls-Universität Heidelberg, Heidelberg, Germany*

[58c]*ZITI Institut für technische Informatik, Ruprecht-Karls-Universität Heidelberg, Mannheim, Germany*

[59]*Faculty of Applied Information Science, Hiroshima Institute of Technology, Hiroshima, Japan*

[60a]*Department of Physics, The Chinese University of Hong Kong, Shatin, N.T., Hong Kong, China*

[60b]*Department of Physics, The University of Hong Kong, Hong Kong, China*

[60c]*Department of Physics, The Hong Kong University of Science and Technology, Clear Water Bay, Kowloon, Hong Kong, China*

[61]*Department of Physics, Indiana University, Bloomington, Indiana, USA*

[62]*Institut für Astro- und Teilchenphysik, Leopold-Franzens-Universität, Innsbruck, Austria*

[63]*University of Iowa, Iowa City, Iowa, USA*

[64]*Department of Physics and Astronomy, Iowa State University, Ames, Iowa, USA*

[65]*Joint Institute for Nuclear Research, JINR Dubna, Dubna, Russia*

[66]*KEK, High Energy Accelerator Research Organization, Tsukuba, Japan*

[67]*Graduate School of Science, Kobe University, Kobe, Japan*

[68]*Faculty of Science, Kyoto University, Kyoto, Japan*

[69]*Kyoto University of Education, Kyoto, Japan*

[70]*Department of Physics, Kyushu University, Fukuoka, Japan*

[71]*Instituto de Física La Plata, Universidad Nacional de La Plata and CONICET, La Plata, Argentina*

[72]*Physics Department, Lancaster University, Lancaster, United Kingdom*

[73a]*INFN Sezione di Lecce, Italy*

[73b]*Dipartimento di Matematica e Fisica, Università del Salento, Lecce, Italy*

[74]*Oliver Lodge Laboratory, University of Liverpool, Liverpool, United Kingdom*

[75]*Department of Physics, Jožef Stefan Institute and University of Ljubljana, Ljubljana, Slovenia*

[76]*School of Physics and Astronomy, Queen Mary University of London, London, United Kingdom*

[77]*Department of Physics, Royal Holloway University of London, Surrey, United Kingdom*

[78]*Department of Physics and Astronomy, University College London, London, United Kingdom*

[79]*Louisiana Tech University, Ruston, Louisiana, USA*

[80]*Laboratoire de Physique Nucléaire et de Hautes Energies, UPMC and Université Paris-Diderot and CNRS/IN2P3, Paris, France*

[81]*Fysiska institutionen, Lunds universitet, Lund, Sweden*

[82]*Departamento de Fisica Teorica C-15, Universidad Autonoma de Madrid, Madrid, Spain*

[83]*Institut für Physik, Universität Mainz, Mainz, Germany*

[84]*School of Physics and Astronomy, University of Manchester, Manchester, United Kingdom*

[85]*CPPM, Aix-Marseille Université and CNRS/IN2P3, Marseille, France*

[86]*Department of Physics, University of Massachusetts, Amherst, Massachusetts, USA*

[87]*Department of Physics, McGill University, Montreal, Quebec, Canada*

[88]*School of Physics, University of Melbourne, Victoria, Australia*

[89]*Department of Physics, The University of Michigan, Ann Arbor, Michigan, USA*

[90]*Department of Physics and Astronomy, Michigan State University, East Lansing, Michigan, USA*

[91a]*INFN Sezione di Milano, Italy*

[91b]*Dipartimento di Fisica, Università di Milano, Milano, Italy*

[92]*B.I. Stepanov Institute of Physics, National Academy of Sciences of Belarus, Minsk, Republic of Belarus*

[93]*National Scientific and Educational Centre for Particle and High Energy Physics, Minsk, Republic of Belarus*

[94]*Department of Physics, Massachusetts Institute of Technology, Cambridge, Massachusetts, USA*

[95]*Group of Particle Physics, University of Montreal, Montreal, Quebec, Canada*

[96]*P.N. Lebedev Institute of Physics, Academy of Sciences, Moscow, Russia*

[97]*Institute for Theoretical and Experimental Physics (ITEP), Moscow, Russia*

[98]*National Research Nuclear University MEPhI, Moscow, Russia*

[99]*D.V. Skobeltsyn Institute of Nuclear Physics, M.V. Lomonosov Moscow State University, Moscow, Russia*

[100]*Fakultät für Physik, Ludwig-Maximilians-Universität München, München, Germany*

[101]*Max-Planck-Institut für Physik (Werner-Heisenberg-Institut), München, Germany*

[102]*Nagasaki Institute of Applied Science, Nagasaki, Japan*

[103]*Graduate School of Science and Kobayashi-Maskawa Institute, Nagoya University, Nagoya, Japan*

[104a]*INFN Sezione di Napoli, Italy*

[104b]*Dipartimento di Fisica, Università di Napoli, Napoli, Italy*

[105]*Department of Physics and Astronomy, University of New Mexico, Albuquerque, New Mexico, USA*

[106]*Institute for Mathematics, Astrophysics and Particle Physics, Radboud University Nijmegen/Nikhef, Nijmegen, Netherlands*

[107]*Nikhef National Institute for Subatomic Physics and University of Amsterdam, Amsterdam, Netherlands*

[108]*Department of Physics, Northern Illinois University, DeKalb, Illinois, USA*

[109]*Budker Institute of Nuclear Physics, SB RAS, Novosibirsk, Russia*

[110]*Department of Physics, New York University, New York, New York, USA*

[111]*Ohio State University, Columbus, Ohio, USA*

[112]*Faculty of Science, Okayama University, Okayama, Japan*

[113]*Homer L. Dodge Department of Physics and Astronomy, University of Oklahoma, Norman, Oklahoma, USA*

[114]*Department of Physics, Oklahoma State University, Stillwater, Oklahoma, USA*

[115]*Palacký University, RCPTM, Olomouc, Czech Republic*

[116]*Center for High Energy Physics, University of Oregon, Eugene, Oregon, USA*

[117]*LAL, Université Paris-Sud and CNRS/IN2P3, Orsay, France*

[118]*Graduate School of Science, Osaka University, Osaka, Japan*

[119]*Department of Physics, University of Oslo, Oslo, Norway*

[120]*Department of Physics, Oxford University, Oxford, United Kingdom*

[121a]*INFN Sezione di Pavia, Italy*

[121b]*Dipartimento di Fisica, Università di Pavia, Pavia, Italy*

[122]*Department of Physics, University of Pennsylvania, Philadelphia, Pennsylvania, USA*

[123]*Petersburg Nuclear Physics Institute, Gatchina, Russia*

[124a]*INFN Sezione di Pisa, Italy*

[124b]*Dipartimento di Fisica E. Fermi, Università di Pisa, Pisa, Italy*

[125]*Department of Physics and Astronomy, University of Pittsburgh, Pittsburgh, Pennsylvania, USA*

[126a]*Laboratorio de Instrumentacao e Fisica Experimental de Particulas - LIP, Lisboa, Portugal*

[126b]*Faculdade de Ciências, Universidade de Lisboa, Lisboa, Portugal*

[126c]*Department of Physics, University of Coimbra, Coimbra, Portugal*

[126d]*Centro de Física Nuclear da Universidade de Lisboa, Lisboa, Portugal*

[126e]*Departamento de Fisica, Universidade do Minho, Braga, Portugal*

[126f]*Departamento de Fisica Teorica y del Cosmos and CAFPE, Universidad de Granada, Granada, Spain*

[126g]*Dep Fisica and CEFITEC of Faculdade de Ciencias e Tecnologia, Universidade Nova de Lisboa, Caparica, Portugal*

[127]*Institute of Physics, Academy of Sciences of the Czech Republic, Praha, Czech Republic*

[128]*Czech Technical University in Prague, Praha, Czech Republic*

[129]*Faculty of Mathematics and Physics, Charles University in Prague, Praha, Czech Republic*

[130]*State Research Center Institute for High Energy Physics, Protvino, Russia*

[131]*Particle Physics Department, Rutherford Appleton Laboratory, Didcot, United Kingdom*

[132a]*INFN Sezione di Roma, Italy*

[132b]*Dipartimento di Fisica, Sapienza Università di Roma, Roma, Italy*

[133a]*INFN Sezione di Roma Tor Vergata, Italy*

[133b]*Dipartimento di Fisica, Università di Roma Tor Vergata, Roma, Italy*

[134a]*INFN Sezione di Roma Tre, Italy*

[134b]*Dipartimento di Matematica e Fisica, Università Roma Tre, Roma, Italy*

[135a]*Faculté des Sciences Ain Chock, Réseau Universitaire de Physique des Hautes Energies-Université Hassan II, Casablanca, Morocco*

[135b]*Centre National de l'Energie des Sciences Techniques Nucleaires, Rabat, Morocco*

[135c]*Faculté des Sciences Semlalia, Université Cadi Ayyad, LPHEA-Marrakech, Morocco*

[135d]*Faculté des Sciences, Université Mohamed Premier and LPTPM, Oujda, Morocco*

[135e]*Faculté des sciences, Université Mohammed V-Agdal, Rabat, Morocco*

[136]*DSM/IRFU (Institut de Recherches sur les Lois Fondamentales de l'Univers), CEA Saclay (Commissariat à l'Energie Atomique et aux Energies Alternatives), Gif-sur-Yvette, France*

[137]*Santa Cruz Institute for Particle Physics, University of California Santa Cruz, Santa Cruz, California, USA*

[138]*Department of Physics, University of Washington, Seattle, Washington, USA*

[139]*Department of Physics and Astronomy, University of Sheffield, Sheffield, United Kingdom*

[140]*Department of Physics, Shinshu University, Nagano, Japan*

[141]*Fachbereich Physik, Universität Siegen, Siegen, Germany*

[142]*Department of Physics, Simon Fraser University, Burnaby, British Columbia, Canada*

[143]*SLAC National Accelerator Laboratory, Stanford, California, USA*

[144a]*Faculty of Mathematics, Physics & Informatics, Comenius University, Bratislava, Slovak Republic*

[144b]*Department of Subnuclear Physics, Institute of Experimental Physics of the Slovak Academy of Sciences, Kosice, Slovak Republic*

[145a]*Department of Physics, University of Cape Town, Cape Town, South Africa*

[145b]*Department of Physics, University of Johannesburg, Johannesburg, South Africa*

[145c]*School of Physics, University of the Witwatersrand, Johannesburg, South Africa*

[146a]*Department of Physics, Stockholm University, Sweden*

[146b]*The Oskar Klein Centre, Stockholm, Sweden*

[147]*Physics Department, Royal Institute of Technology, Stockholm, Sweden*

[148]*Departments of Physics & Astronomy and Chemistry, Stony Brook University, Stony Brook, New York, USA*

[149]*Department of Physics and Astronomy, University of Sussex, Brighton, United Kingdom*

[150]*School of Physics, University of Sydney, Sydney, Australia*

[151]*Institute of Physics, Academia Sinica, Taipei, Taiwan*

[152]*Department of Physics, Technion: Israel Institute of Technology, Haifa, Israel*

[153]*Raymond and Beverly Sackler School of Physics and Astronomy, Tel Aviv University, Tel Aviv, Israel*

[154]*Department of Physics, Aristotle University of Thessaloniki, Thessaloniki, Greece*

[155]*International Center for Elementary Particle Physics and Department of Physics, The University of Tokyo, Tokyo, Japan*

[156]*Graduate School of Science and Technology, Tokyo Metropolitan University, Tokyo, Japan*

[157]*Department of Physics, Tokyo Institute of Technology, Tokyo, Japan*

[158]*Department of Physics, University of Toronto, Toronto, Ontario, Canada*

[159a]*TRIUMF, Vancouver, British Columbia, Canada*

[159b]*Department of Physics and Astronomy, York University, Toronto, Ontario, Canada*

[160]*Faculty of Pure and Applied Sciences, University of Tsukuba, Tsukuba, Japan*

[161]*Department of Physics and Astronomy, Tufts University, Medford, Massachusetts, USA*

[162]*Centro de Investigaciones, Universidad Antonio Narino, Bogota, Colombia*

[163]*Department of Physics and Astronomy, University of California Irvine, Irvine, California, USA*

[164a]*INFN Gruppo Collegato di Udine, Sezione di Trieste, Udine, Italy*

[164b]*ICTP, Trieste, Italy*

[164c]*Dipartimento di Chimica, Fisica e Ambiente, Università di Udine, Udine, Italy*

[165]*Department of Physics, University of Illinois, Urbana, Illinois, USA*

[166]*Department of Physics and Astronomy, University of Uppsala, Uppsala, Sweden*

[167]*Instituto de Física Corpuscular (IFIC) and Departamento de Física Atómica, Molecular y Nuclear and Departamento de Ingeniería Electrónica and Instituto de Microelectrónica de Barcelona (IMB-CNM), University of Valencia and CSIC, Valencia, Spain*

[168]*Department of Physics, University of British Columbia, Vancouver, British Columbia, Canada*

[169]*Department of Physics and Astronomy, University of Victoria, Victoria, British Columbia, Canada*

[170]*Department of Physics, University of Warwick, Coventry, United Kingdom*

[171]*Waseda University, Tokyo, Japan*

[172]*Department of Particle Physics, The Weizmann Institute of Science, Rehovot, Israel*

[173]*Department of Physics, University of Wisconsin, Madison, Wisconsin, USA*

[174]*Fakultät für Physik und Astronomie, Julius-Maximilians-Universität, Würzburg, Germany*

[175]*Fachbereich C Physik, Bergische Universität Wuppertal, Wuppertal, Germany*

[176]*Department of Physics, Yale University, New Haven, Connecticut, USA*

[177]*Yerevan Physics Institute, Yerevan, Armenia*

[178]*Centre de Calcul de l'Institut National de Physique Nucléaire et de Physique des Particules (IN2P3), Villeurbanne, France*

[a]Also at Department of Physics, King's College London, London, United Kingdom.

[b]Also at Institute of Physics, Azerbaijan Academy of Sciences, Baku, Azerbaijan.

[c]Also at Novosibirsk State University, Novosibirsk, Russia.

[d]Also at TRIUMF, Vancouver, British Columbia, Canada.

[e]Also at Department of Physics, California State University, Fresno, California, USA.

[f]Also at Department of Physics, University of Fribourg, Fribourg, Switzerland.

[g]Also at Departamento de Fisica e Astronomia, Faculdade de Ciencias, Universidade do Porto, Portugal.

[h]Also at Tomsk State University, Tomsk, Russia.

[i]Also at CPPM, Aix-Marseille Université and CNRS/IN2P3, Marseille, France.

[j]Also at Università di Napoli Parthenope, Napoli, Italy.

[k]Also at Institute of Particle Physics (IPP), Canada.

[l]Also at Particle Physics Department, Rutherford Appleton Laboratory, Didcot, United Kingdom.

[m]Also at Department of Physics, St. Petersburg State Polytechnical University, St. Petersburg, Russia.

[n]Also at Louisiana Tech University, Ruston, Louisiana, USA.

[o]Also at Institucio Catalana de Recerca i Estudis Avancats, ICREA, Barcelona, Spain.

[p]Also at Department of Physics, National Tsing Hua University, Taiwan.

[q]Also at Department of Physics, The University of Texas at Austin, Austin, Texas, USA.

[r]Also at Institute of Theoretical Physics, Ilia State University, Tbilisi, Georgia.

[s]Also at CERN, Geneva, Switzerland.

[t]Also at Georgian Technical University (GTU),Tbilisi, Georgia.

[u]Also at Ochadai Academic Production, Ochanomizu University, Tokyo, Japan.

[v]Also at Manhattan College, New York, New York, USA.

[w]Also at Institute of Physics, Academia Sinica, Taipei, Taiwan.

[x]Also at LAL, Université Paris-Sud and CNRS/IN2P3, Orsay, France.

[y]Also at Academia Sinica Grid Computing, Institute of Physics, Academia Sinica, Taipei, Taiwan.

[z]Also at School of Physics, Shandong University, Shandong, China.

[aa]Also at Moscow Institute of Physics and Technology State University, Dolgoprudny, Russia.

[ab]Also at Section de Physique, Université de Genève, Geneva, Switzerland.

[ac]Also at International School for Advanced Studies (SISSA), Trieste, Italy.

[ad]Also at Department of Physics and Astronomy, University of South Carolina, Columbia, South Carolina, USA.

[ae]Also at School of Physics and Engineering, Sun Yat-sen University, Guangzhou, China.

[af]Also at Faculty of Physics, M.V. Lomonosov Moscow State University, Moscow, Russia.

[ag]Also at National Research Nuclear University MEPhI, Moscow, Russia.

[ah]Also at Department of Physics, Stanford University, Stanford, California, USA.

[ai]Also at Institute for Particle and Nuclear Physics, Wigner Research Centre for Physics, Budapest, Hungary.

[aj]Also at Department of Physics, The University of Michigan, Ann Arbor, Michigan, USA.

[ak]Also at Discipline of Physics, University of KwaZulu-Natal, Durban, South Africa.

[al]Also at University of Malaya, Department of Physics, Kuala Lumpur, Malaysia.

[*]Deceased.